IEEE Access
Multidisciplinary | Rapid Review | Open Access Journal

Received September 25, 2019, accepted October 16, 2019, date of publication October 23, 2019, date of current version November 4, 2019.

Digital Object Identifier 10.1109/ACCESS.2019.2949081

Cognitive Multihop Wireless Powered Relaying Networks Over Nakagami-*m* Fading Channels

TOAN-VAN NGUYEN [1] **AND BEONGKU AN** [2]
[1]Department of Electronics and Computer Engineering, Hongik University, Sejong 30016, South Korea
[2]Department of Software and Communications Engineering, Hongik University, Sejong 30016, South Korea

Corresponding author: Beongku An (beongku@hongik.ac.kr)

This work was supported in part by the Basic Science Research Program through the National Research Foundation of Korea (NRF), Ministry of Education, under Grant (No. 2016R1D1A1B03934898) and in part by the National Research Foundation of Korea (NRF) Grant funded by the Korea government (MSIT) (No. 2019R1A2C1083996).

ABSTRACT In this paper, we study the end-to-end performance of multi-hop wireless powered relaying networks cognitively operating with primary networks over Nakagami-*m* fading channels. Our analysis considers multi-hop wireless powered relaying systems in which all communication nodes harvest energy from a multiple antennas power beacon (PB) to transmit data to multiple destinations in the presence of a multiple antennas primary receiver (PR). Aiming at improving end-to-end system performance, we propose two relay selection schemes, namely data channel based relay selection (DbRS) and interference channel based relay selection (IbRS), under cognitive radio approach. By taking into account the harvested energy and the interference power constraint, we derive the exact closed-form expression for the outage probability (OP) of the proposed schemes, which is then verified by Monte Carlo simulations over Nakagami-*m* fading channels. The tractable asymptotic OP of each scheme is also provided unveiling several important insights on system characteristics and performance trends. Moreover, we develop the asymptotic upper bounds for the ergodic capacity and bit error rate (BER) of the considered multi-hop relaying network. Numerical results in terms of system OP, ergodic capacity, and average BER performance are provided to demonstrate that DbRS scheme outperforms IbRS one, which by its turn outperforms random relay selection scheme. Finally, the influences of the number of antennas at PB and PR, number of relays in each cluster, number of hops, the PB and PR placements, and time switching ratio on the overall system performance are examined and discussed comprehensively.

INDEX TERMS Cognitive radio networks, energy harvesting, multi-hop networks, Nakagami-*m* fading channel, outage probability, power beacon, relay selection, ergodic capacity, BER.

I. INTRODUCTION

Energy harvesting (EH) in cognitive radio networks has recently considered as a promising solution in the upcoming era of the Internet of Things (IoT) due to its efficiency both on spectrum and energy [1], [2]. In cognitive radio networks (CRNs), secondary users are allowed to operate on the same frequency spectrum of primary users at any time as long as interference from secondary transmitters received at primary receivers (PRs) below the maximum allowable interference defined by its target quality of service thus improving the overall system spectral efficiency [3], [4]. Wireless energy harvesting offers great convenience to wireless users since radio frequency (RF) signals have been widely used as a vehicle for wireless information and energy transmission [5].

Recently, cooperative cognitive networks have been attracted attention by the research community to improve network performance and extend network coverage, e.g., see [6]–[9]. In particular, Duong *et. al.* studied the impact of primary interference from multiple primary transceivers on performance of secondary networks (SN) [6]. By combining the direct link and cooperative links, Bao *et. al.* proposed cognitive decode-and-forward (DF) networks to improve secondary network coverage [7]. To provide full spatial diversity, Yeoh *et. al.* in [8] proposed a cognitive multiple-input multiple-output (MIMO) network, where users in primary and secondary networks are equipped with multiple antennas. Very recently, a wireless energy harvesting and information transfer protocol in cognitive relay networks

The associate editor coordinating the review of this manuscript and approving it for publication was Ahmed Mohamed Ahmed Almradi.

This work is licensed under a Creative Commons Attribution 4.0 License. For more information, see http://creativecommons.org/licenses/by/4.0/

has been developed, where a secondary transmitter scavenges energy from the received primary signal and then employs the harvested energy to forward the resulting signals along with the secondary signal. The paper also analytically derived the exact expressions of the outage probabilities for both primary and secondary networks [9]. For achieving high energy requirement and extending the propagation range of wireless power transfer in large scale cognitive radio networks, the dedicated power beacons (PB) are usually employed for wireless networks with many functions such as channel estimation, spectrum sensing and digital beam-forming techniques. In practice, the power beacon is integrated to the dedicated base station to power mobile devices within short propagation ranges [10]. The authors in [11] considered the wireless powered communication networks (WPCNs), where the power beacon is equipped with multiple antennas and employs beamforming technique to improve the energy transfer efficiency. To enhance the achievable network throughput in WPCNs, the authors in [12] proposed "harvest then transmit" protocol by jointly optimizing power allocation and time-sharing among nodes to maximize the overall network throughput. Since the RF signal can convey both information and energy, the simultaneous wireless information and power transfer (SWIPT) has recently growing attention by research community. The practical receiver mechanism for SWIPT systems was designed in [13] to improve the energy transfer and information rate. SWIPT based cooperative relay networks have also been extensively studied in [14], [15]. Specifically, Nasir *et. al.* in [14] introduced the time switching relaying (TSR) and power switching relaying (PSR) mechanisms for amplify-and-forward (AF) EH cooperative relaying networks and showed that the network throughput of TSR is better than that of PSR methods at high transmission rates. For increasing the network diversity gain, the authors in [15] analyzed EH incremental DF relaying systems employing maximal ratio combining (MRC) technique at destination.

Beside cooperative communications, multi-hop relaying is an effective approach considered for cognitive networks. In particular, Bao *et. al.* studied the effect of imperfect channel state information (CSI) on the performance of cognitive multi-hop networks [16]. In [17], two interference cancellation approaches under various MIMO schemes were proposed to improve the performance of multi-hop secondary networks. In [18], a max-min relay selection in multi-hop CRNs was introduced to improve the spatial gain for the last hop transmission. A novel underlay cognitive radio network for short range communication was studied in [19], where a single-hop secondary network coexists with multi-hop primary networks. Furthermore, the system outage probability (OP) of secondary and primary networks were derived to show the significant influence of the number of hops on the primary networks and the positive effect of interference cancellation on the secondary networks at high average signal-to-noise ratios (SNRs). However, all above mentioned research works have not focused on energy harvesting. Recently, Xu *et. al.* in [20] proposed underlay cognitive multi-hop relay networks, where secondary users (SUs) can harvest the energy from the dedicated power beacon to support the data transmission. As an extension of [20], the paper [21] considered an accumulate energy harvesting model applied for multi-hop network under cognitive radio paradigm. However, the sub-time slots for energy harvesting and data transmission were designed unequally making it difficult for synchronization and serve collisions possibly occurring in the cognitive multi-hop networks. More recently, the authors in [22] introduced an EH-cognitive multi-hop network based on time division multiple access (TDMA) with equal sub-time slots for data transmission in Rayleigh fading environments. Over Nakagami-*m* fading channels, a novel multi-hop relaying network was proposed in [23], where the relay nodes harvest energy from external co-channel interferences for their operation. However, the aforementioned works only limited on a single cooperative relay in EH underlay cognitive multi-hop networks with inefficient data transmission. To enhance the transmission reliability for EH multi-hop cooperative networks, the authors in [24] proposed the various relay selection methods applied for each two-hop in multi-hop cluster-based relay networks over Nakagami-*m* fading channels. In the practical perspective, the choice of Nakagami-*m* fading channel is more general that fully provides the properties of channel transmission. Very recently, the performance evaluation of multi-hop cluster-based relay networks over Nakagami-*m* fading channels has been investigated in [25], and the outage probability analysis of multi-hop relaying scheme in cognitive radio networks has been conducted in [26], accounting for multiple antennas at both the primary transmitter and receiver. However, the asymptotic analysis for the network performance were not provided in the previous works, which poses a difficulty to draw out any insight into the network behaviors. Moreover, to the best of our knowledge, there is no closed-form expression for the ergodic capacity and average BER in these works because of the theoretical intractability of its analysis. In this paper, we come up with new steps to derive the tight upper bound expressions for the ergodic capacity and bit error rate of the multi-hop wireless powered relaying networks, which comprehensively provides a general framework to evaluate the overall system performance under cognitive radio constraints.

In this paper, we study the end-to-end performance analysis of cognitive multi-hop wireless powered relaying networks with energy beamforming over Nakagami-*m* fading channels. Making use of Nakagami-*m* fading channel can characterize more versatile fading scenarios that accurately reflects the natures of wireless environments. Our analysis accounts for cluster-based relays and multiple antennas at both the power beacon and primary receiver. Multiple destination nodes are also deployed to achieve the diversity gain as well as the reception reliability. Relay selection is applied at each hop which not only improves the transmission reliability of secondary multi-hop networks but also alleviates the undesirable interference to the primary networks. The random relay selection (RS) scheme is provided as a baseline scheme for comparison purposes. Our main contributions are as follows:

- We propose the data channel based relay selection (DbRS) and interference channel based relay selection (IbRS) schemes to improve the end-to-end outage performance for cognitive wireless powered multi-hop relaying networks. Specifically, DbRS scheme outperforms IbRS scheme, which is raised as an efficient scheme for multi-hop transmission.
- We derive the exact closed-form expressions for the outage probability of the proposed schemes over Nakagami-m fading channels and validate by using Monte-Carlo simulation. To provide further insights about how the primary receiver positions affect the secondary multi-hop network performance, we analyze the outage probability under two conditions which are near and far scenarios.
- We continue to derive the ergodic capacity and average BER from the obtained asymptotic analysis in the far scenario which serve as the performance bound of secondary multi-hop network.
- We show through the numerical results that the system OP can be significantly improved by increasing the number of antennas at PB and the number of relays in each cluster. Moreover, the system characteristics and performance trends can be unfolded completely through the asymptotic results of outage probability, which is very useful for network planning and design.

The rest of the paper will be arranged as follows. Section II-A describes the system model of proposed scheme. The outage performance analysis is described in Section III and the simulation results are evaluated in Section IV. Finally, Section V concludes the paper.

Mathematical Notations and Functions: x and $\mathbf{x}$ are presented the scalar x and vector $\mathbf{x}$, respectively. $[\mathbf{x}]_i$ denotes the ith element of a vector $\mathbf{x}$, $\|.\|$ is the Euclidean norm, $(.)^H$ is the Hermitian operator. Pr[.] symbolizes probability, $f_X(.)$ and $F_X(.)$ denote the probability density function (PDF) and cumulative distribution function (CDF) of random variable X, respectively. $\Gamma(.)$ represents the Gamma function [27, Eq. 8.310.1], $W_{u,v}(.)$ indicates the Whittaker function [28, Eq. 13.1.33], $G^{c,d}_{a,b}[.|.]$ stands for the Meijer's G-function [27, Eq. 9.301], and $K_v(.)$ designates the v-order modified Bessel function of second kind [28, Eq. 9.6.22].

II. SYSTEM MODEL

A. SYSTEM DESCRIPTION

We consider a cognitive multi-hop wireless powered relaying system, where the secondary network and primary network share the same frequency licensed band in a geographical area of interest, as illustrated in Fig. 1. An $L-$antennas primary receiver in the primary network[1] employs maximal ratio

[1]We mainly focus on the cognitive multi-hop wireless powered relaying system and its performance under interference power constraint, considering the effect of primary interference is thus beyond the scope of this paper.

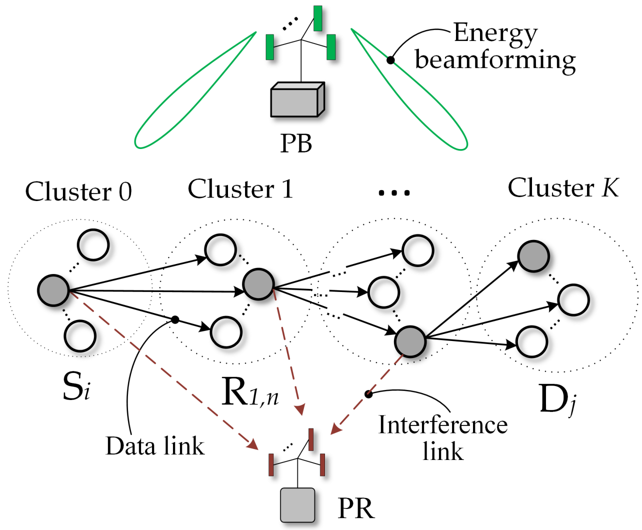

FIGURE 1. A cognitive multi-hop wireless powered relaying network.

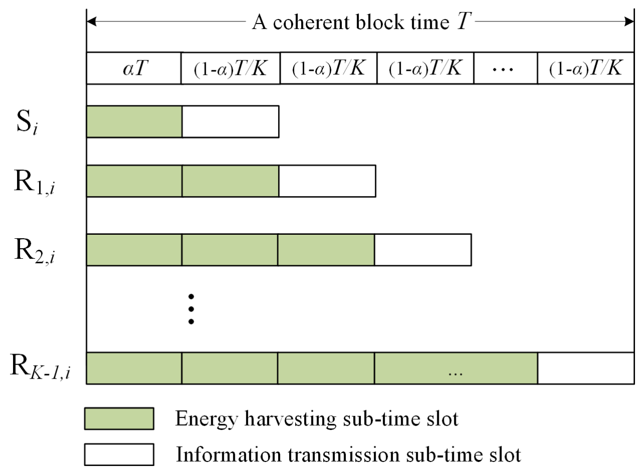

FIGURE 2. The time block structure for accumulate energy harvesting and information transmission phases.

combining (MRC) technique to combine its received signals. In the secondary network, $(K-1)$ intermediate relay clusters are deployed to assist N_0 sources S_i, $i \in \{1, \ldots, N_0\}$ to forward the data to N_K destinations $\mathsf{D}_j, j \in \{1, \ldots, N_K\}$ through multi-hop decode-and-forward relaying protocol. A relay node, $\mathsf{R}_{k,n}$, presents the n^{th} relay in k^{th} cluster belonging to a set of relays $\mathcal{R} = \{\mathsf{R}_{k,n}|k = 0, \ldots, K, n = 1, \ldots, N_k\}$, where N_k denotes the number of nodes in the k^{th} cluster. Note that $\mathsf{R}_{0,i} \equiv \mathsf{S}_i$ and $\mathsf{R}_{K,j} \equiv \mathsf{D}_j$. We assume that all communication nodes have limited power supply, and they rely on external energy charging from an $M-$antennas power beacon (PB) through energy beamforming. Moreover, sources and all relay nodes are equipped with single antenna and operate on half-duplex mode. The proposed system can be realized in many practical applications such as cellular networks, wireless sensor networks, IoT systems, vehicle tracking and roadside facilities. The channel notations used in this paper are given in Table 1.

TABLE 1. Summary of main notations.

Channel Notation	Definition
$g_{m,k,i}$	The channel coefficient from mth antenna at PB to $\mathsf{R}_{k,i}$, where $m \in \{1,\ldots,M\}$.
$h_{k,i,j}$	The channel coefficient from $\mathsf{R}_{k,i}$ to $\mathsf{R}_{k+1,j}$.
$f_{k,i,l}$	The channel coefficient from $\mathsf{R}_{k,i}$ to lth antenna at PR, where $l \in \{1,\ldots,L\}$.
$\|g_{m,k,i}\|^2$	The channel gain from mth antenna at PB to $\mathsf{R}_{k,i}$.
$\|h_{k,i,j}\|^2$	The channel gain from $\mathsf{R}_{k,i}$ to $\mathsf{R}_{k+1,j}$.
$\|f_{k,i,l}\|^2$	The channel gain from $\mathsf{R}_{k,i}$ to lth antenna at PR.
$d_{\mathsf{PB},k}$	The distance (in meter) between PB and $\mathsf{R}_{k,i}$.
$d_{\mathsf{R},k}$	The distance (in meter) between $\mathsf{R}_{k,i}$ and $\mathsf{R}_{k+1,j}$.
$d_{\mathsf{PR},k}$	The distance (in meter) between $\mathsf{R}_{k,i}$ and PR.
$\lambda_{\mathsf{PB},k}$, $\lambda_{\mathsf{R},k}$, $\lambda_{\mathsf{PR},k}$	Parameters of i.i.d. Nakagami-m distributions.
α	The time switching ratio.
$\eta \in (0,1]$	The energy conversion efficiency.
P	The transmit power of PB
β	The pathloss exponent.
m_1, m_2, m_3	Nakagami-m fading parameter with integer values.
d_0	The reference distance.
$\mathcal{L}$	The measured pathloss at d_0.
σ^2	Noise variance.
$\mathcal{P}_{out}^{\mathrm{S}}$	The outage probability of proposed schemes.

The perfect knowledge of CSI is supposed to be available at each receiver node. Also, all channels are assumed to experience quasi-static independent identically distributed (i.i.d.) Nakagami-m fading channels. As a result, the channel gains, i.e., $|g_{m,k,i}|^2$, $|h_{k,i,j}|^2$ and $|f_{k,i,l}|^2$, follow gamma distribution with parameter, respectively, as $\lambda_{\mathsf{PB},k} = \mathcal{L}(d_{\mathsf{PB},k}/d_0)^\beta$, $\lambda_{\mathsf{R},k} = \mathcal{L}(d_{\mathsf{R},k}/d_0)^\beta$ and $\lambda_{\mathsf{PR},k} = \mathcal{L}(d_{\mathsf{PR},k}/d_0)^\beta$. The system operation is divided into two consecutive phases including energy harvesting (EH) and information transmission phases which will be described in detail next.

B. ENERGY HARVESTING PHASE

In the EH phase, considering time switching (TS) architecture, we propose the *harvest and accumulate* protocol for the energy model in cognitive multi-hop relaying networks, where the latter relays have more time for harvesting energy than the former ones, as illustrated in Fig. 2. In particular, all communication nodes simultaneously harvest energy from the power beacon in the first sub-time slot of αT, wherein $\alpha \in (0,1]$ is the time switching ratio and T denotes the coherent transmission block. The remaining time, i.e., $(1-\alpha)T$, can be divided equally in K orthogonal sub-time slots for K hops transmission, thanks to the time-division-multiple-access in medium access control layer [29]. The latter relay nodes continuously harvest and accumulate energy before their turns to transmit data, where the accumulated energy is temporarily stored in a super-capacitor and latter completely consumed for information transmission [14], [30]. The last sub-time slot at each relay, i.e., $(1-\alpha)T/K$, is always preserved for the information transmission. Without loss of generality, the period time for harvesting and accumulating energy at the relay $\mathsf{R}_{k,i}$ can be expressed as $\alpha T + k(1-\alpha)T/K$. The PB is equipped with multiple antennas and employs energy beamforming to improve energy transfer efficiency. Thus, the harvested energy at relay $\mathsf{R}_{k,i}$ can be expressed as

$$E_k = \eta(\alpha + k(1-\alpha)/K)TP|\mathbf{w}\mathbf{g}_k^H|^2, \tag{1}$$

where $\mathbf{w} \triangleq [\mathbf{w}_m]_{m\in M}$ and $\mathbf{g}_k \triangleq [g_{m,k,i}]_{m\in M}$ present the energy beamforming vector and the channel coefficient vector from the PB to $\mathsf{R}_{k,i}$, respectively. Based on [11], [31], we consider $\mathbf{w} = \mathbf{g}_k/\|\mathbf{g}_k\|$ in this paper.

C. INFORMATION TRANSMISSION PHASE

The information transmission phase is occurred during the period of $(1-\alpha)T/K$. From (1), the transmit power of $\mathsf{R}_{k,i}$ over the information transmission period can be presented as

$$P_k^E = \chi_k P|\mathbf{w}\mathbf{g}_k^H|^2 \overset{(a)}{=} \chi_k P\|\mathbf{g}_k\|^2, \tag{2}$$

where (a) is obtained by recalling $\mathbf{w} = \mathbf{g}_k/\|\mathbf{g}_k\|$, and $\chi_k \triangleq \eta(\alpha K/(1-\alpha)+k)$.

In cognitive underlay mode, the interference power received at the primary receiver from secondary transmitters must be lower than the peak interference power constraint, i.e., I_p, to protect the primary communication [4]. Since PR is equipped with L antennas and employs MRC technique, the maximum transmit power of relay $\mathsf{R}_{k,i}$ can be determined as

$$P_k^I = \frac{I_p}{\sum_{l=1}^L |f_{k,i,l}|^2}. \tag{3}$$

From (2) and (3), the transmit power constraint at $\mathsf{R}_{k,i}$ is constrained as

$$P_k = \min\left(\chi_k P\|\mathbf{g}_k\|^2, \frac{I_p}{\sum_{l=1}^L |f_{k,i,l}|^2}\right). \tag{4}$$

The instantaneous SNR for hop k can be expressed as

$$\gamma_k = \min\left(\chi_k \bar{\gamma}_P\|\mathbf{g}_k\|^2, \frac{\bar{\gamma}_I}{\sum_{l=1}^L |f_{k,i,l}|^2}\right)|h_{k,i,j}|^2, \tag{5}$$

where $\bar{\gamma}_P = P/\sigma^2$ and $\bar{\gamma}_I = I_p/\sigma^2$.

The relay selection strategies will be presented in the next subsection to show how to improve the considered system performance.

D. RELAY SELECTION SCHEMES

1) RANDOM RELAY SELECTION

We consider the random relay selection scheme as a benchmark scheme for comparison purposes. Due to the simplicity of the RS scheme, it can be easily implemented in practice. The RS scheme randomly selects a relay in each cluster for multi-hop communication; thus, the instantaneous SNR at hop k can be expressed as

$$\gamma_k^{\mathrm{RS}} = \min\left(\chi_k \bar{\gamma}_P\|\mathbf{g}_k\|^2, \frac{\bar{\gamma}_I}{\sum_{l=1}^L |f_{k,i,l}|^2}\right)|h_{k,i^*,j^*}|^2, \tag{6}$$

It is noted that the RS scheme does not require any CSI for selecting the next forwarder.

2) INTERFERENCE CHANNEL BASED RELAY SELECTION

At each cluster, relay selection scheme is employed, i.e., the relay having the lowest interference channel gain from the primary receiver is chosen to be the forwarder of the next hop. The IbRS scheme aims to mitigate the effect of unwanted interference to the primary receiver as well as protect the primary network operation. We denote the best relay at cluster $k+1$ as R_{k+1,j^*}, the selected relay at the cluster k is chosen by the following strategy

$$\mathsf{R}_{k,i^*} = \arg\max_{i=1,\ldots,N_k} \min\left(\chi_k\bar{\gamma}_P\|\mathbf{g}_k\|^2, \frac{\bar{\gamma}_I}{\sum_{l=1}^{L}|f_{k,i,l}|^2}\right)|h_{k,i,j^*}|^2. \quad (7)$$

From (7), the corresponding instantaneous SNR received at hop k can be expressed as

$$\gamma_k^{\text{IbRS}} = \min\left(\chi_k\bar{\gamma}_P\|\mathbf{g}_k\|^2, \frac{\bar{\gamma}_I}{\min\limits_{i=1,\ldots,N_k}\sum_{l=1}^{L}|f_{k,i,l}|^2}\right)|h_{k,i,j^*}|^2. \quad (8)$$

3) DATA CHANNEL BASED RELAY SELECTION

At each cluster, relay selection scheme is employed, i.e., the relay having the highest data channel gain from the transmitter is chosen to be the forwarder of the next hop. The DbRS scheme aims to enhance the diversity data transmission for multi-hop relaying networks. We denote the best relay at cluster k as R_{k,i^*}, the selected relay at the cluster $k+1$ is chosen by the following strategy

$$\mathsf{R}_{k+1,i^*} = \arg\max_{j=1,\ldots,N_{k+1}} \min \times\left(\chi_k\bar{\gamma}_P\|\mathbf{g}_k\|^2, \frac{\bar{\gamma}_I}{\sum_{l=1}^{L}|f_{k,i^*,l}|^2}\right)|h_{k,i^*,j}|^2, \quad (9)$$

where σ^2 is the noise variance.

The corresponding instantaneous SNR received at hop $k+1$ can be expressed as

$$\gamma_k^{\text{DbRS}} = \max_{j=1,\ldots,N_{k+1}} \min\left(\chi_k\bar{\gamma}_P\|\mathbf{g}_k\|^2, \frac{\bar{\gamma}_I}{\sum_{l=1}^{L}|f_{k,i^*,l}|^2}\right)|h_{k,i^*,j}|^2. \quad (10)$$

III. PERFORMANCE ANALYSIS

In this section, we analyze the performance of multi-hop relaying network in the presence of a multiple antennas PR. In particular, the performance metrics including outage probability, ergodic capacity and average BER are derived for the multi-hop relaying network. Moreover, the asymptotic analysis of cognitive multi-hop system under different scenarios are also provided to reveal some important insights into the network behaviors and characteristics.

A. EXACT OUTAGE PROBABILITY

In this subsection, we will derive the exact and asymptotic expression for the system outage probability of the proposed system over Nakagami-*m* fading channels. Using DF relaying, the system outage probability can be defined as the probability that the information rate falls below a predefined target data rate (R_{th}), which is mathematically written as follows [16], [17]:

$$\mathcal{P}_{\text{out}}^{\mathtt{Sch}} = \Pr\left[\frac{1-\alpha}{K}\log_2\left(1+\min_{k=1,\ldots,K}\gamma_k^{\mathtt{Sch}}\right) < R_{th}\right], \quad (11)$$

where $\mathtt{Sch} \in \{\text{RS, IbRS, DbRS}\}$, R_{th} bits/s/Hz is the target data rate and the pre-factor of $(1-\alpha)/K$ is accounted for the information transmission for K hops.

$$\begin{aligned}\mathcal{P}_{\text{out}}^{\text{RS}} &= 1-\prod_{k=1}^{K}\Bigg[\sum_{t=0}^{m_2-1}\frac{2\Xi_k^{\frac{(m_1M+t)}{2}}}{t!\Gamma(m_1M)}K_{m_1M-t}\left(2\sqrt{\Xi_k}\right)+\sum_{v=0}^{m_3L-1}\frac{2}{v!\Gamma(m_1M)}\Bigg[\Theta_k^{\frac{m_1M+v}{2}}K_{m_1M-v}\left(2\sqrt{\Theta_k}\right)-\sum_{t=0}^{m_2-1}\frac{\Xi_k^t\Theta_k^v}{t!}\\&\times\left(\Xi_k+\Theta_k\right)^{\frac{m_1M-v-t}{2}}K_{m_1M-v-t}\left(2\sqrt{\Xi_k+\Theta_k}\right)\Bigg]-\sum_{q=0}^{m_1M-1}\frac{2}{q!\Gamma(m_3L)}\Bigg[\Theta_k^{\frac{m_3L+q}{2}}K_{m_3L-q}\left(2\sqrt{\Theta_k}\right)-\sum_{t=0}^{m_2-1}\frac{1}{t!}\\&\times\Theta_k^{m_3L}\Xi_k^t\left(\Xi_k+\Theta_k\right)^{\frac{q-m_3L-t}{2}}K_{m_3L+t-q}\left(2\sqrt{\Xi_k+\Theta_k}\right)\Bigg]\Bigg],\end{aligned} \quad (12)$$

$$\begin{aligned}\mathcal{P}_{\text{out}}^{\text{IbRS}} &= 1-\prod_{k=1}^{K}\Bigg[\sum_{v=0}^{N_k(m_3L-1)}\frac{2b_v^{N_k}N_k^{\frac{m_1M-v}{2}}}{\Gamma(m_1M)}\Theta_k^{\frac{m_1M+v}{2}}K_{m_1M-v}\left(2\sqrt{N_k\Theta_k}\right)+\sum_{u=0}^{m_2-1}\frac{2\Xi_k^{\frac{m_1M+u}{2}}}{u!\Gamma(m_1M)}K_{m_1M-u}\left(2\sqrt{\Xi_k}\right)\\&-\sum_{u=0}^{m_2-1}\sum_{v=0}^{N_k(m_3L-1)}\frac{2b_v^{N_k}\Xi_k^u\Theta_k^v}{u!\Gamma(m_1M)}\left(\Xi_k+N_k\Theta_k\right)^{\frac{m_1M-u-v}{2}}K_{m_1M-v-u}\left(2\sqrt{\Xi_k+N_k\Theta_k}\right)-\sum_{t=0}^{m_1M-1}\sum_{v=0}^{(N_k-1)(m_3L-1)}\frac{b_v^{N_k}}{t!}\\&\times\frac{2}{\Gamma(m_3L)}N_k^{\frac{2-m_3L-v+t}{2}}\Theta_k^{\frac{m_3L+v+t}{2}}K_{m_3L+v-t}\left(2\sqrt{N_k\Theta_k}\right)+\sum_{t=0}^{m_1M-1}\sum_{u=0}^{m_2-1}\sum_{v=0}^{(N_k-1)(m_3L-1)}\frac{2N_kb_v^{N_k-1}\Xi_k^u\Theta_k^{m_3L+v}}{t!u!\Gamma(m_3L)}\\&\times\left(\Xi_k+N_k\Theta_k\right)^{\frac{t-m_3L-u-v}{2}}K_{m_3L+v+u-t}\left(2\sqrt{\Xi_k+N_k\Theta_k}\right)\Bigg].\end{aligned} \quad (13)$$

1) RANDOM RELAY SELECTION

From (6), the OP of RS scheme can be obtained by the following theorem.

Theorem 1: The exact closed-form expression for the OP of RS scheme over Nakagami-*m* fading channels can be derived as (12), as shown at the bottom of the previous page, where $\gamma_{\text{th}} = 2^{\frac{KR_{th}}{1-\alpha}} - 1$,

$$\Xi_k = \frac{m_1\lambda_{E,k} m_2\lambda_{D,k}\gamma_{\text{th}}}{\chi_k\bar{\gamma}_P}, \text{ and } \Theta_k = \frac{m_1\lambda_{E,k} m_3\lambda_{I,k}\bar{\gamma}_I}{\chi_k\bar{\gamma}_P}.$$

Proof: The proof of Theorem 1 is in Appendix A. ∎

2) INTERFERENCE CHANNEL BASED RELAY SELECTION

From (8), the OP of IbRS scheme can be obtained by the following theorem.

Theorem 2: The exact closed-form expression for the OP of IbRS scheme over Nakagami-*m* fading channels can be derived as (13), as shown at the bottom of the previous page.

Proof: First, the OP of the IbRS scheme can be equivalently rewritten from (11) as

$$\mathcal{P}_{\text{out}}^{\text{IbRS}} = 1 - \prod_{k=1}^{K}\left[1 - F_{\gamma_k^{\text{IbRS}}}(\gamma_{\text{th}})\right]. \tag{14}$$

Considering the instantaneous SNR γ_k^{IbRS} in (8), we denote $X = \|\mathbf{g}_k\|^2$, $Y = |h_{k,i,j^*}|^2$, and $Z_i^* = \min_{i=1,\ldots,N_k} \sum_{l=1}^{L} |f_{k,i,l}|^2$.

It is challenging to determine the CDF and PDF of Z_i^* since it is shown as a minimum of a sum of gamma distributed random variables (RVs). The following lemma is important since it provides the closed-form expressions for the CDF and PDF of Z_i^*.

Lemma 1: The CDF and PDF of Z_i^* can be derived, respectively, as

$$F_{Z_i^*}(x) = 1 - \exp(-m_3\lambda_{I,k}N_k x) \sum_{v=0}^{N_k(m_3L-1)} \frac{(m_3\lambda_{I,k}x)^v}{t!} b_v^{N_k}, \tag{15}$$

$$f_{Z_i^*}(x) = \exp(-m_3\lambda_{I,k}N_k x) \sum_{v=0}^{(N_k-1)(m_3L-1)} x^{m_3L+v-1} \times N_k (m_3\lambda_{I,k})^{m_3L+v}\Gamma(m_3L)^{-1} b_v^{N_k-1}, \tag{16}$$

where the coefficients $b_v^{N_k}$ can be expressed as

$$b_0^{N_k} = 1,\ b_1^{N_k} = N_k,\ b_{N_k(m_2-1)}^{N_k} = [(m_2-1)!]^{-N_k},$$
$$b_v^{N_k} = \frac{1}{v}\sum_{j=1}^{J} \frac{j(N_k+1)-v}{j!} b_{v-j}^{N_k},$$
$$J = \min(v, m_2-1),\ 2 \le v \le N_k(m_2-1)-1. \tag{17}$$

The proof of Lemma 1 is in Appendix B. The CDF and PDF of Z_i^* in (15) and (16) have an exponential form with recursive parameters $b_v^{N_k}$ and $b_v^{N_k-1}$, respectively, making them become mathematical tractability. We shall soon see that such forms will play a significant role in simplifying the evaluation of system performance over Nakagami-*m* fading channels.

We now turn our attention to the calculation of the CDF of γ_k^{IbRS} which can be written as

$$F_{\gamma_k^{\text{RS}}}(\gamma_{\text{th}}) = \underbrace{\Pr[\chi_k\bar{\gamma}_P X < \bar{\gamma}_I/Z_i^*, \chi_k\bar{\gamma}_P XY < \gamma_{\text{th}}]}_{I_3} + \underbrace{\Pr[\chi_k\bar{\gamma}_P X > \bar{\gamma}_I/Z_i^*, \bar{\gamma}_I Y/Z_i^* < \gamma_{\text{th}}]}_{I_4}. \tag{18}$$

In order to obtain $F_{\gamma_k^{\text{IbRS}}}(\gamma_{\text{th}})$, we need to calculate I_3 and I_4. By invoking the concepts of probability theory [32], I_3 can be rewritten as

$$I_3 = \int_0^\infty F_{Z_i^*}\Big(\frac{\bar{\gamma}_I}{\chi_k\bar{\gamma}_P x}\Big) F_Y\Big(\frac{\gamma_{\text{th}}}{\chi_k\bar{\gamma}_P x}\Big) f_X(x)dx. \tag{19}$$

Invoking Lemma 1, the CDF of Z_i^* can be easily obtained. Then, plugging $f_X(\cdot)$, $F_Y(\cdot)$, and $F_{Z_i^*}(\cdot)$ into (19), along with the help of [27, Eq. (3.471.9)] and after some manipulations, the closed-form expression of I_3 can be obtained as

$$\begin{aligned} I_3 = 1 &- \sum_{v=0}^{N_k(m_3L-1)} \frac{2b_v^{N_k}}{\Gamma(m_1M)} \Big(\frac{m_1\lambda_{E,k}m_3\lambda_{I,k}\bar{\gamma}_I}{\chi_k\bar{\gamma}_P}\Big)^{\frac{m_1M+v}{2}} \\ &\times N_k^{\frac{m_1M-v}{2}} K_{m_1M-v}\Big(2\sqrt{\frac{m_1\lambda_{E,k}m_3\lambda_{I,k}N_k\bar{\gamma}_I}{\chi_k\bar{\gamma}_P}}\Big) \\ &- \sum_{u=0}^{m_2-1} \frac{2}{u!\Gamma(m_1M)} \Big(\frac{m_1\lambda_{E,k}m_2\lambda_{D,k}\gamma_{\text{th}}}{\chi_k\bar{\gamma}_P}\Big)^{\frac{m_1M+u}{2}} \\ &\times K_{m_1M-u}\Big(2\sqrt{\frac{m_1\lambda_{E,k}m_2\lambda_{D,k}\gamma_{\text{th}}}{\chi_k\bar{\gamma}_P}}\Big) + \sum_{u=0}^{m_2-1}\frac{2}{u!} \\ &\times \sum_{v=0}^{N_k(m_3L-1)} \frac{b_v^{N_k}}{\Gamma(m_1M)} \Big(\frac{m_1\lambda_{E,k}}{\chi_k\bar{\gamma}_P}\Big)^{\frac{m_1M+v+u}{2}} \\ &\times \frac{(m_3\lambda_{I,k}N_k\bar{\gamma}_I + m_2\lambda_{D,k}\gamma_{\text{th}})^{\frac{m_1M-v-u}{2}}}{(m_3\lambda_{I,k}\bar{\gamma}_I)^{-v}(m_2\lambda_{D,k}\gamma_{\text{th}})^{-u}} \\ &\times K_{m_1M-v-u}\Big(2\sqrt{\frac{m_3\lambda_{I,k}N_k\bar{\gamma}_I + m_2\lambda_{D,k}\gamma_{\text{th}}}{(m_1\lambda_{E,k})^{-1}\chi_k\bar{\gamma}_P}}\Big). \end{aligned} \tag{20}$$

We are now in a position to derive I_4, which can be calculated as

$$I_4 = \int_0^\infty \Big[1 - F_X\Big(\frac{\bar{\gamma}_I}{\chi_k\bar{\gamma}_P x}\Big)\Big] F_Y\Big(\frac{\gamma_{\text{th}}x}{\bar{\gamma}_I}\Big) f_{Z_i^*}(x)dx. \tag{21}$$

Recalling again Lemma 1, the PDF of Z_i^* can be easily obtained. Then, substituting $F_X(\cdot)$, $f_{Z_i^*}(\cdot)$ and $F_Y(\cdot)$ into (21), along with the help of [27, Eq. (3.471.9)] and after some manipulations, I_4 can be obtained as

$$\begin{aligned} I_4 = &\sum_{t=0}^{m_1M-1}\sum_{v=0}^{(N_k-1)(m_3L-1)} \Big(\frac{m_1\lambda_{E,k}m_3\lambda_{I,k}\bar{\gamma}_I}{\chi_k\bar{\gamma}_P}\Big)^{\frac{m_3L+t+v}{2}} \\ &\times \frac{2N_k^{\frac{2-m_3L-v+t}{2}}}{b_v^{1-N_k}\Gamma(m_3L)t!} K_{m_3L+v-t}\Big(2\sqrt{\frac{m_1\lambda_{E,k}m_3\lambda_{I,k}N_k\bar{\gamma}_I}{\chi_k\bar{\gamma}_P}}\Big) \end{aligned}$$

$$-\sum_{u=0}^{m_2-1}\frac{(m_3\lambda_{I,k}\bar{\gamma}_I+m_2\lambda_{D,k}\gamma_{\rm th})^{\frac{t-m_3L-u}{2}}}{(m_3\lambda_{I,k}\bar{\gamma}_I)^{-m_3L}(m_2\lambda_{D,k}\gamma_{\rm th})^{-u}}\Big(\frac{m_1\lambda_{E,k}}{\chi_k\bar{\gamma}_P}\Big)^{\frac{m_3L+u+t}{2}}$$
$$\times\frac{1}{u!}K_{m_3L+u-t}\Big(2\sqrt{\frac{m_3\lambda_{I,k}\bar{\gamma}_I+m_2\lambda_{D,k}\gamma_{\rm th}}{(m_1\lambda_{E,k})^{-1}\chi_k\bar{\gamma}_P}}\Big). \quad (22)$$

Finally, by substituting I_3 and I_4 into (18), we can obtain the desired OP as (13). The proof of Theorem 2 is concluded. ■

3) DATA CHANNEL BASED RELAY SELECTION

From (10), the OP of DbRS scheme can be obtained by the following theorem.

Theorem 3: The exact closed-form expression for the OP of DbRS scheme over Nakagami-*m* fading channels can be derived as (23), as shown at the bottom of this page.

Proof: From (11), the OP of the DbRS scheme can be rewritten as

$$\mathcal{P}_{\rm out}^{\rm DbRS}=1-\prod_{k=1}^{K}\big[1-F_{\gamma_k^{\rm DbRS}}(\gamma_{\rm th})\big] \quad (24)$$

For the sake of notational convenience, let $X=\|\mathbf{g}_k\|^2$, $Y_j^*=\max_{j=1,\ldots,N_k}|h_{k,i^*,j}|^2$, and $Z=\sum_{l=1}^{L}|f_{k,i,l}|^2$. Recalling that Y_j^* is the maximum of N_k i.i.d. gamma distributed RVs, thus the CDF of Y_j^* can be derived by invoking Lemma 1 as

$$F_{Y_j^*}(x)=\sum_{n=0}^{N_k}\sum_{t=0}^{n(m_2-1)}(-1)^n\binom{N_k}{n}b_t^n(m_2\lambda_{D,k}x)^t\times\exp(-nm_2\lambda_{D,k}x)$$
$$=1+\sum_{n=1}^{N_k}\sum_{t=0}^{n(m_2-1)}(-1)^n\binom{N_k}{n}b_t^n(m_2\lambda_{D,k}x)^t\times\exp(-nm_2\lambda_{D,k}x), \quad (25)$$

where b_t^n denotes the recursive coefficient, as shown in (17).

From (10), the CDF of $\gamma_k^{\rm DbRS}$ can be rewritten as

$$F_{\gamma_k^{\rm DbRS}}(\gamma_{\rm th})=\underbrace{\Pr[\chi_k\bar{\gamma}_PX<\bar{\gamma}_I/Z,\,\chi_k\bar{\gamma}_PXY_{j^*}<\gamma_{\rm th}]}_{I_5}+\underbrace{\Pr[\chi_k\bar{\gamma}_PX>\bar{\gamma}_I/Z,\,\bar{\gamma}_IY_{j^*}/Z<\gamma_{\rm th}]}_{I_6}. \quad (26)$$

In order to obtain $F_{\gamma_k^{\rm DbRS}}(\gamma_{\rm th})$, we need to calculate I_5 and I_6. We first consider I_5 which can be expressed as

$$I_5=\int_0^\infty F_Z\Big(\frac{\bar{\gamma}_I}{\chi_k\bar{\gamma}_Px}\Big)F_{Y_{j^*}}\Big(\frac{\gamma_{\rm th}}{\chi_k\bar{\gamma}_Px}\Big)f_X(x)dx, \quad (27)$$

Then, plugging $F_Z(\cdot)$, $f_X(\cdot)$, and $F_{Y_{j^*}}(\cdot)$ into (27), along with the help of [27, Eq. (3.471.9)] and after some manipulations, the closed-form expression of I_5 can be obtained as

$$I_5=1-\sum_{v=0}^{m_3L-1}\frac{2}{v!\Gamma(m_1M)}\Big(\frac{m_1\lambda_{E,k}m_3\lambda_{I,k}\bar{\gamma}_I}{\chi_k\bar{\gamma}_P}\Big)^{\frac{m_1M+v}{2}}\times K_{m_1M-v}\Big(2\sqrt{\frac{m_1\lambda_{E,k}m_3\lambda_{I,k}\bar{\gamma}_I}{\chi_k\bar{\gamma}_P}}\Big)+\sum_{n=1}^{N_k}(-1)^n\binom{N_k}{n}$$
$$\times\sum_{t=0}^{n(m_2-1)}\frac{2b_t^nn^{\frac{m_1M-t}{2}}}{\Gamma(m_1M)}\Big(\frac{m_1\lambda_{E,k}m_2\lambda_{D,k}\gamma_{\rm th}}{\chi_k\bar{\gamma}_P}\Big)^{\frac{m_1M+t}{2}}\times K_{m_1M-t}\Big(2\sqrt{\frac{m_1\lambda_{E,k}nm_2\lambda_{D,k}\gamma_{\rm th}}{\chi_k\bar{\gamma}_P}}\Big)-\sum_{v=0}^{m_3L-1}\frac{2}{v!}$$
$$\times\sum_{n=1}^{N_k}\sum_{t=0}^{n(m_2-1)}\binom{N_k}{n}\frac{(-1)^nb_v^{N_k}}{\Gamma(m_1M)}\Big(\frac{m_1\lambda_{E,k}}{\chi_k\bar{\gamma}_P}\Big)^{\frac{m_1M+v+t}{2}}\times\frac{(m_3\lambda_{I,k}\bar{\gamma}_I+nm_2\lambda_{D,k}\gamma_{\rm th})^{\frac{m_1M-v-t}{2}}}{(m_3\lambda_{I,k}\bar{\gamma}_I)^{-v}(m_2\lambda_{D,k}\gamma_{\rm th})^{-t}}$$
$$\times K_{m_1M-v-t}\Big(2\sqrt{\frac{m_3\lambda_{I,k}N_k\bar{\gamma}_I+m_2\lambda_{D,k}\gamma_{\rm th}}{(m_1\lambda_{E,k})^{-1}\chi_k\bar{\gamma}_P}}\Big). \quad (28)$$

We are now in a position to derive I_6, which can be calculated as

$$I_6=\int_0^\infty\Big[1-F_X\Big(\frac{\bar{\gamma}_I}{\chi_k\bar{\gamma}_Px}\Big)\Big]F_{Y_{j^*}}\Big(\frac{\gamma_{\rm th}x}{\bar{\gamma}_I}\Big)f_Z(x)dx. \quad (29)$$

Substituting $F_X(\cdot)$, $f_Z(\cdot)$ and $F_{Y_{j^*}}(\cdot)$ into (29), along with the help of [27, Eq. (3.471.9)] and after some manipulations, I_6 can be obtained as

$$I_6=\sum_{t=0}^{m_1M-1}\sum_{n=0}^{N_k}\sum_{v=0}^{n(m_2-1)}\frac{(-1)^n}{t!}\binom{N_k}{n}\Big(\frac{m_1\lambda_{E,k}}{\chi_k\bar{\gamma}_P}\Big)^{\frac{m_3L+v+t}{2}}\times\frac{2b_v^n(m_3\lambda_{I,k}\bar{\gamma}_I+nm_2\lambda_{D,k}\gamma_{\rm th})^{\frac{t-m_3L-v}{2}}}{\Gamma(m_3L)(m_3\lambda_{I,k}\bar{\gamma}_I)^{-m_3L}(m_2\lambda_{D,k}\gamma_{\rm th})^{-v}}$$
$$\times K_{m_3L+v-t}\Big(2\sqrt{\frac{m_3\lambda_{I,k}\bar{\gamma}_I+nm_2\lambda_{D,k}\gamma_{\rm th}}{(m_1\lambda_{E,k})^{-1}\chi_k\bar{\gamma}_P}}\Big). \quad (30)$$

$$\mathcal{P}_{\rm out}^{\rm DbRS}=1-\prod_{k=1}^{K}\Bigg[\sum_{v=0}^{m_3L-1}\frac{2}{v!\Gamma(m_1M)}\Theta_k^{\frac{m_1M+v}{2}}K_{m_1M-v}\big(2\sqrt{\Theta_k}\big)+\sum_{n=1}^{N_k}\sum_{t=0}^{n(m_2-1)}\frac{2b_t^n(-1)^n}{n^t\Gamma(m_1M)}\binom{N_k}{n}K_{m_1M-t}\big(2\sqrt{n\Xi_k}\big)$$
$$\times(n\Xi_k)^{\frac{m_1M+t}{2}}+\sum_{v=0}^{m_3L-1}\sum_{n=1}^{N_k}\sum_{t=0}^{n(m_2-1)}\frac{2b_t^n(-1)^n}{v!\Gamma(m_1M)}\binom{N_k}{n}\Xi^t\Theta_k^v(\Theta_k+n\Xi_k)^{\frac{m_1M-v-t}{2}}K_{m_1M-v-t}\big(2\sqrt{\Theta_k+n\Xi_k}\big)$$
$$-\sum_{u=0}^{m_1M-1}\sum_{n=0}^{N_k}\sum_{t=0}^{n(m_2-1)}\frac{2(-1)^nb_t^n}{u!\Gamma(m_3L)}\binom{N_k}{n}\Xi_k^t\Theta_k^{m_3L}(\Theta_k+n\Xi_k)^{\frac{u-m_3L-t}{2}}K_{m_3L+t-u}\big(2\sqrt{\Theta_k+n\Xi_k}\big)\Bigg]. \quad (23)$$

Finally, by substituting I_5 and I_6 into (26), we can obtain the desired OP as (23). The proof of Theorem 3 is concluded. ■

B. ASYMPTOTIC OUTAGE PROBABILITY

In this subsection, we derive the asymptotic expressions for the OP of three schemes in two deployment scenarios. Specifically, the far scenario is consistent with the PR located very far from the secondary multi-hop relaying network corresponding to $I_p \to \infty$. The near scenario can be seen as the PR placement nearby the secondary multi-hop relaying network corresponding to $P \to \infty$. Each scenario plays as a performance bound to the proposed cognitive system setup. From (4), the transmit power P_k can be rewritten as

$$P_{k,i} = \min\left(\chi_k P\|\mathbf{g}_k\|^2, \frac{I_p}{\sum_{l=1}^{L}|f_{k,i,l}|^2}\right), \approx \begin{cases} \chi_k P\|\mathbf{g}_k\|^2, & \text{if } I_p \to \infty, \\ \frac{I_p}{\sum_{l=1}^{L}|f_{k,i,l}|^2}, & \text{if } P \to \infty. \end{cases} \quad (31)$$

1) RANDOM RELAY SELECTION

Theorem 4: The asymptotic expression for the outage floor of RS scheme with near and far scenarios can be derived as

$$\mathcal{P}_{\text{asym}}^{\text{RS}} \approx \begin{cases} \sum_{k=1}^{K} F_{\gamma_{k,\text{F}}^{\text{RS}}}, & \text{if } I_p \to \infty, \\ \sum_{k=1}^{K} F_{\gamma_{k,\text{N}}^{\text{RS}}}, & \text{if } P \to \infty, \end{cases} \quad (32)$$

where $F_{\gamma_{k,\text{F}}^{\text{RS}}}$ and $F_{\gamma_{k,\text{N}}^{\text{RS}}}$ are given, respectively, as

$$F_{\gamma_{k,\text{F}}^{\text{RS}}} = 1 - \sum_{t=0}^{m_2-1} \frac{2}{\Gamma(m_1 M)t!}\left(\frac{m_1\lambda_{E,k} m_2 \lambda_{D,k}\gamma_{\text{th}}}{\chi_k \bar{\gamma}_P}\right)^{\frac{m_1 M+t}{2}} \times K_{m_1 M-t}\left(2\sqrt{\frac{m_1\lambda_{E,k} m_2\lambda_{D,k}\gamma_{\text{th}}}{\chi_k\bar{\gamma}_P}}\right), \quad (33)$$

$$F_{\gamma_{k,\text{N}}^{\text{RS}}} = 1 - \sum_{t=0}^{m_2-1} \frac{\Gamma(m_3 L+t)(m_3\lambda_{I,k}\bar{\gamma}_I)^{m_3 L}(m_2\lambda_{D,k}\gamma_{\text{th}})^t}{t!\Gamma(m_3 L)(m_2\lambda_{D,k}\gamma_{\text{th}} + m_3\lambda_{I,k}\bar{\gamma}_I)^{m_3 L+t}}. \quad (34)$$

Proof: The proof of Theorem 4 is in Appendix C. ■

2) INTERFERENCE CHANNEL BASED RELAY SELECTION

In IbRS scheme, when the PR is located very far from the multi-hop network in far scenario, the interference links may disappear resulting in the inactivity of relay selection criterion (7) on the far scenario. Thus, asymptotic analysis of IbRS scheme in far scenario is similar to that of the RS scheme which will be presented in the following Theorem.

Theorem 5: The asymptotic expression for the OP of IbRS scheme with near and far scenarios can be derived as

$$\mathcal{P}_{\text{asym}}^{\text{IbRS}} \approx \begin{cases} \sum_{k=1}^{K} F_{\gamma_{k,\text{F}}^{\text{IbRS}}}, & \text{if } I_p \to \infty, \\ \sum_{k=1}^{K} F_{\gamma_{k,\text{N}}^{\text{IbRS}}}, & \text{if } P \to \infty, \end{cases} \quad (35)$$

where $F_{\gamma_{k,\text{F}}^{\text{IbRS}}}$ and $F_{\gamma_{k,\text{N}}^{\text{IbRS}}}$ are given, respectively, as

$$F_{\gamma_{k,\text{F}}^{\text{IbRS}}} = F_{\gamma_{k,\text{F}}^{\text{RS}}}, \quad (36)$$

$$F_{\gamma_{k,\text{N}}^{\text{IbRS}}} = \sum_{v=0}^{(N_k-1)(m_3L-1)} \frac{\Gamma(m_3L+v)b_v^{N_k-1}}{\Gamma(m_3L)} N_k^{1-m_3L-v} - \sum_{v=0}^{(N_k-1)(m_3L-1)}\sum_{u=0}^{m_2-1} \frac{N_k b_v^{N_k-1}}{\Gamma(m_3L)u!}\left(\frac{m_2\lambda_{D,k}\gamma_{\text{th}}}{\bar{\gamma}_I}\right)^u \times (m_3\lambda_{I,k})^{m_3L+v}\Gamma(m_3L+v+u) \times \left(m_3\lambda_{I,k}N_k + \frac{m_2\lambda_{D,k}\gamma_{\text{th}}}{\bar{\gamma}_I}\right)^{-m_3L-v-u}. \quad (37)$$

Proof: The proof of Theorem 5 is in Appendix D. ■

3) DATA CHANNEL BASED RELAY SELECTION

Theorem 6: The asymptotic expression for the outage floor of DbRS scheme with near and far scenarios can be derived as

$$\mathcal{P}_{\text{asym}}^{\text{DbRS}} \approx \begin{cases} \sum_{k=1}^{K} F_{\gamma_{k,\text{F}}^{\text{DbRS}}}, & \text{if } I_p \to \infty, \\ \sum_{k=1}^{K} F_{\gamma_{k,\text{N}}^{\text{DbRS}}}, & \text{if } P \to \infty, \end{cases} \quad (38)$$

where $F_{\gamma_{k,\text{F}}^{\text{DbRS}}}$ and $F_{\gamma_{k,\text{N}}^{\text{DbRS}}}$ are given, respectively, as

$$F_{\gamma_{k,\text{F}}^{\text{DbRS}}} = 1 + \sum_{n=1}^{N_k}\sum_{t=0}^{n(m_2-1)} \binom{N_k}{n}\left(\frac{m_1\lambda_{E,k} n m_2\lambda_{D,k}\gamma_{\text{th}}}{\chi_k\bar{\gamma}_P}\right)^{\frac{m_1M+t}{2}} \times \frac{2(-1)^n b_t^n}{\Gamma(m_1M)n^t} K_{m_1M-t}\left(2\sqrt{\frac{m_1\lambda_{E,k} n m_2\lambda_{D,k}\gamma_{\text{th}}}{\chi_k\bar{\gamma}_P}}\right), \quad (39)$$

$$F_{\gamma_{k,\text{N}}^{\text{DbRS}}} = 1 + \sum_{n=1}^{N_k}\sum_{t=0}^{n(m_2-1)} \binom{N_k}{n} \frac{(-1)^n b_t^n \Gamma(m_3L+t)}{\Gamma(m_3L)(m_3\lambda_{I,k})^{-m_3L}} \times \left(\frac{m_2\lambda_{D,k}\gamma_{\text{th}}}{\bar{\gamma}_I}\right)^t \left(m_3\lambda_{I,k} + \frac{n m_2\lambda_{D,k}\gamma_{\text{th}}}{\bar{\gamma}_I}\right)^{-m_3L-t}. \quad (40)$$

Proof: The proof of Theorem 6 is in Appendix E. ■

C. ERGODIC CAPACITY ANALYSIS

In this subsection, we derive close-form expressions for the ergodic capacity of the proposed schemes in far scenario which implies that the considered system is operating on non-cognitive radio mode. Moreover, the ergodic capacity analysis in far scenario can be seen as the upper bound capacity performance of the proposed cognitive system. The ergodic capacity of the secondary multi-hop network can be defined as [16]

$$C_{\texttt{Sch}} = \frac{1-\alpha}{K}\mathbb{E}[\log_2(1+\gamma_{e2e})] = \frac{1-\alpha}{K\log(2)}\int_0^{+\infty}\frac{1-F_{\gamma_{e2e}}(x)}{1+x}dx \quad (41)$$

where $F_{\gamma_{e2e}}(x)$ denotes the CDF of the end-to-end SNR of multi-hop network. Based on the min-cut max-flow theorem [33], [34], the end-to-end capacity of the system can not be larger than that of each individual link, which can be upper bounded as

$$C_{\mathtt{Sch}} \le C_{\mathtt{Sch}}^{\mathrm{Up}} = \frac{1-\alpha}{K} \min_{k=1,\ldots,K} \mathbb{E}[\log_2(1+\gamma_k^{\mathtt{Sch}})], \quad (42)$$

where $C_{\mathtt{Sch}}^{\mathrm{Up}}$ is the upper bound ergodic capacity of the proposed schemes.

1) RANDOM RELAY SELECTION

Theorem 7: The asymptotic closed-form expression for the ergodic capacity of the RS scheme over Nakagami-m fading channels can be devised as

$$C_{\mathrm{RS}}^{\mathrm{Up}} = \min_{k=1,\ldots,K} (C_k^{\mathrm{RS}}), \quad (43)$$

where

$$C_k^{\mathrm{RS}} = \sum_{t=0}^{m_2-1} \frac{(1-\alpha)\chi_k \bar{\gamma}_P}{t! K \log(2)\Gamma(m_1 M) m_1 \lambda_{E,k} m_2 \lambda_{D,k}} \times G_{3,1}^{1,3}\left(\frac{\chi_k \bar{\gamma}_P}{m_1 \lambda_{E,k} m_2 \lambda_{D,k}} \middle| \begin{matrix} -m_1 M & -t & 0 \\ & 0 & \end{matrix} \right). \quad (44)$$

Proof: The ergodic capacity of each individual link in multi-hop secondary network can be expressed as

$$C_k^{\mathrm{RS}} = \frac{1-\alpha}{K\log(2)} \int_0^{+\infty} \frac{1 - F_{\gamma_{k,\mathrm{F}}^{\mathrm{RS}}}(x)}{1+x} dx. \quad (45)$$

Plugging (33), i.e., with respect to x, into (45), it follows that

$$C_k^{\mathrm{RS}} = \sum_{t=0}^{m_2-1} \frac{2(1-\alpha)}{t! K \log(2)\Gamma(m_1 M)} \int_0^{+\infty} \frac{1}{1+x} \times \left(\frac{m_1 \lambda_{E,k} m_2 \lambda_{D,k} x}{\chi_k \bar{\gamma}_P} \right)^{\frac{m_1 M + t}{2}} \times K_{m_1 M - t}\left(2\sqrt{\frac{m_1 \lambda_{E,k} m_2 \lambda_{D,k} x}{\chi_k \bar{\gamma}_P}} \right) dx. \quad (46)$$

The integral in (46) can be solved by using the following equation [27, Eq. (8.3.2.21)]

$$\frac{1}{1+x} = G_{1,1}^{1,1}\left(x \middle| \begin{matrix} 0 \\ 0 \end{matrix} \right). \quad (47)$$

Substituting (47) into (46) with the help of [27, Eq. (7.821.3)], we obtain C_k^{RS} as (44). The proof is concluded. ■

2) INTERFERENCE CHANNEL BASED RELAY SELECTION

In this scheme, the asymptotic expression for the OP in far scenario is similar to that of RS scheme, as shown in (36). Therefore, the ergodic capacity of each individual link in IbRS scheme is the same as RS scheme, which was calculated as (44). The end-to-end ergodic capacity of IbRS scheme and can be obtained by the following corollary.

Corollary 1: The ergodic capacity of IbRS scheme in far scenario can be expressed as

$$C_{\mathrm{IbRS}}^{\mathrm{Up}} = \min_{k=1,\ldots,K} (C_k^{\mathrm{IbRS}}), \quad (48)$$

where $C_k^{\mathrm{IbRS}} = C_k^{\mathrm{RS}}$.

3) DATA CHANNEL BASED RELAY SELECTION

Theorem 8: The asymptotic closed-form expression for the ergodic capacity of the DbRS scheme over Nakagami-m fading channels can be devised as

$$C_{\mathrm{DbRS}}^{\mathrm{Up}} = \min_{k=1,\ldots,K} (C_k^{\mathrm{DbRS}}), \quad (49)$$

where

$$C_k^{\mathrm{DbRS}} = -\sum_{t=0}^{n(m_2-1)} \sum_{n=1}^{N_k} \binom{N_k}{n} \frac{(-1)^n n^{-t-1} b_t^n (1-\alpha)}{K \ln(2)\Gamma(m_1 M) m_1 \lambda_{E,k}} \times \frac{\chi_k \bar{\gamma}_P}{m_2 \lambda_{D,k}} G_{3,1}^{1,3}\left(\frac{\chi_k \bar{\gamma}_P}{m_1 \lambda_{E,k} n m_2 \lambda_{D,k}} \middle| \begin{matrix} -m_1 M & -t & 0 \\ & 0 & \end{matrix} \right). \quad (50)$$

Proof: The ergodic capacity of each individual link in secondary multi-hop network can be expressed as

$$C_k^{\mathrm{DbRS}} = \frac{1-\alpha}{K\log(2)} \int_0^{+\infty} \frac{1 - F_{\gamma_{k,\mathrm{F}}^{\mathrm{DbRS}}}(x)}{1+x} dx. \quad (51)$$

Plugging (39), i.e., with respect to x, into (51), it follows that

$$C_k^{\mathrm{DbRS}} = -\sum_{t=0}^{n(m_2-1)} \sum_{n=1}^{N_k} (-1)^n \binom{N_k}{n} \frac{2(1-\alpha) b_t^n n^{-t}}{K \log(2)\Gamma(m_1 M)} \times \int_0^{+\infty} \frac{1}{1+x} \left(\frac{m_1 \lambda_{E,k} n m_2 \lambda_{D,k} x}{\chi_k \bar{\gamma}_P} \right)^{\frac{m_1 M + t}{2}} \times K_{m_1 M - t}\left(2\sqrt{\frac{m_1 \lambda_{E,k} n m_2 \lambda_{D,k} x}{\chi_k \bar{\gamma}_P}} \right) dx. \quad (52)$$

By applying (47) into (52), along with the help of [27, Eq. (7.821.3)], we obtain C_k^{DbRS} as (50). The proof is concluded. ■

D. BIT ERROR RATE ANALYSIS

In this subsection, we derive closed-form expressions for the average BER of proposed schemes over Nakagami-m fading channels. Instead of using the well-know moment generating function, we adopt an alternative approach for the calculation of the average BER that shows its simplicity and tractability. By invoking a general form of average BER from [35, Eq. 20] for the proposed multi-hop network as follows:

$$\mathrm{BER}_{\mathtt{Sch}} = \frac{\theta\sqrt{\vartheta}}{2\sqrt{\pi}} \int_0^{+\infty} \frac{\exp(-bx)}{\sqrt{x}} F_{e2e}(x) dx, \quad (53)$$

where θ and ϑ are modulation-specific constants. Such modulation parameters include binary phase-shift keying modulation (BPSK) ($\theta = 1, \vartheta = 1$), or binary frequency shift keying (BFSK) ($\theta = 1, \vartheta = 0.5$) [35].

1) RANDOM RELAY SELECTION

Theorem 9: The asymptotic closed-form expression for the average BER of the RS scheme over Nakagami-m fading channels can be devised as

$$\begin{aligned}
&\mathrm{BER}_{\mathrm{RS}}^{\mathrm{Up}} \\
&\approx \theta\sqrt{\vartheta}\Bigg[\frac{K}{2}-\sum_{k=1}^{K}\sum_{t=0}^{m_2-1}\frac{\Gamma(1/2+m_1M)\Gamma(1/2+t)}{2t!\Gamma(m_1M)\sqrt{\pi}} \\
&\times\left(\frac{m_1\lambda_{E,k}m_2\lambda_{D,k}}{\chi_k\bar{\gamma}_P}\right)^{\frac{m_1M+t-1}{2}}\exp\left(\frac{m_1\lambda_{E,k}m_2\lambda_{D,k}}{2\chi_k\bar{\gamma}_P}\right) \\
&\times W_{-\frac{m_1M+t}{2},\frac{m_1M-t}{2}}\left(\frac{m_1\lambda_{E,k}m_2\lambda_{D,k}}{\chi_k\bar{\gamma}_P}\right)\Bigg]. \qquad (54)
\end{aligned}$$

Proof: By using (33), we rewrite the CDF of $F_{e2e,\mathrm{RS}}^{\mathrm{Up}}(x)$ under the following form

$$\begin{aligned}
&F_{e2e,\mathrm{RS}}^{\mathrm{Up}}(x) \\
&= K-\sum_{k=1}^{K}\sum_{t=0}^{m_2-1}\frac{2}{t!}\left(\frac{m_1\lambda_{E,k}m_2\lambda_{D,k}x}{\chi_k\bar{\gamma}_P}\right)^{\frac{m_1M+t}{2}} \\
&\times\frac{1}{\Gamma(m_1M)}K_{m_1M-t}\left(2\sqrt{\frac{m_1\lambda_{E,k}m_2\lambda_{D,k}x}{\chi_k\bar{\gamma}_P}}\right). \qquad (55)
\end{aligned}$$

Substituting (55) into (53), which yields

$$\begin{aligned}
&\mathrm{BER}_{\mathrm{RS}}^{\mathrm{Up}} \\
&= \frac{\theta\sqrt{\vartheta}K}{2}-\sum_{k=1}^{K}\sum_{t=0}^{m_2-1}\frac{\theta\sqrt{\vartheta}}{t!\Gamma(m_1M)\sqrt{\pi}} \\
&\times\left(\frac{m_1\lambda_{E,k}m_2\lambda_{D,k}}{\chi_k\bar{\gamma}_P}\right)^{\frac{m_1M+t}{2}}\int_0^\infty x^{\frac{m_1M+t-1}{2}} \\
&\times\exp(-x)K_{m_1M-t}\left(2\sqrt{\frac{m_1\lambda_{E,k}m_2\lambda_{D,k}x}{\chi_k\bar{\gamma}_P}}\right)dx. \qquad (56)
\end{aligned}$$

By changing variable $y=\sqrt{x}$, equation (56) can be expressed as

$$\begin{aligned}
&\mathrm{BER}_{\mathrm{RS}}^{\mathrm{Up}} \\
&= \frac{\theta\sqrt{\vartheta}K}{2}-\sum_{k=1}^{K}\sum_{t=0}^{m_2-1}\frac{\theta\sqrt{\vartheta}}{t!\Gamma(m_1M)\sqrt{\pi}} \\
&\times\left(\frac{m_1\lambda_{E,k}m_2\lambda_{D,k}}{\chi_k\bar{\gamma}_P}\right)^{\frac{m_1M+t}{2}}\int_0^\infty y^{m_1M+t} \\
&\times\exp(-y^2)K_{m_1M-t}\left(2y\sqrt{\frac{m_1\lambda_{E,k}m_2\lambda_{D,k}}{\chi_k\bar{\gamma}_P}}\right)dy. \qquad (57)
\end{aligned}$$

By applying [27, Eq. (6.631.3)] for the corresponding integrals in (57), we can obtain the desired result as (54), and finish the proof here. ■

2) INTERFERENCE CHANNEL BASED RELAY SELECTION

In this scheme, the asymptotic expression for the OP in far scenario is similar to that of RS scheme resulting in the same analytical result for average BER. Thus, the end-to-end average BER of IbRS scheme and can be obtained by the following corollary.

Corollary 2: The asymptotic closed-form expression for the average BER of IbRS scheme in far scenario can be expressed as

$$\mathrm{BER}_{\mathrm{IbRS}}^{\mathrm{Up}} = \mathrm{BER}_{\mathrm{RS}}^{\mathrm{Up}}, \qquad (58)$$

where $\mathrm{BER}_{\mathrm{RS}}^{\mathrm{Up}}$ is expressed as (54).

3) DATA CHANNEL BASED RELAY SELECTION

Theorem 10: The asymptotic closed-form expression for the average BER of the DbRS scheme over Nakagami-*m* fading channels can be devised as

$$\begin{aligned}
&\mathrm{BER}_{\mathrm{DbRS}}^{\mathrm{Up}} \\
&\approx \theta\sqrt{\vartheta}\Bigg[\frac{K}{2}+\sum_{k=1}^{K}\sum_{n=1}^{N_k}\sum_{t=0}^{n(m_2-1)}\binom{N_k}{n}\frac{(-1)^n b_t^n}{2\Gamma(m_1M)} \\
&\times\Gamma(1/2+m_1M)\left(\frac{m_1\lambda_{E,k}nm_2\lambda_{D,k}}{\chi_k\bar{\gamma}_P}\right)^{\frac{m_1M+t-1}{2}} \\
&\times\Gamma(1/2+t)\exp\left(\frac{m_1\lambda_{E,k}nm_2\lambda_{D,k}}{2\chi_k\bar{\gamma}_P}\right)\frac{n^{-t}}{\sqrt{\pi}} \\
&\times W_{-\frac{m_1M+t}{2},\frac{m_1M-t}{2}}\left(\frac{m_1\lambda_{E,k}nm_2\lambda_{D,k}}{\chi_k\bar{\gamma}_P}\right)\Bigg]. \qquad (59)
\end{aligned}$$

Proof: By using (39), the CDF of $F_{e2e,\mathrm{DbRS}}^{\mathrm{Up}}(x)$ can be expressed under the following form

$$\begin{aligned}
F_{e2e,\mathrm{DbRS}}^{\mathrm{Up}}(x) &= K+\sum_{k=1}^{K}\sum_{t=0}^{n(m_2-1)}\sum_{n=1}^{N_k}(-1)^n\binom{N_k}{n}2b_t^n \\
&\times\frac{n^{-t}}{\Gamma(m_1M)}\left(\frac{m_1\lambda_{E,k}nm_2\lambda_{D,k}x}{\chi_k\bar{\gamma}_P}\right)^{\frac{m_1M+t}{2}} \\
&\times K_{m_1M-t}\left(2\sqrt{\frac{m_1\lambda_{E,k}nm_2\lambda_{D,k}x}{\chi_k\bar{\gamma}_P}}\right). \qquad (60)
\end{aligned}$$

Substituting (60) into (53), which yields

$$\begin{aligned}
\mathrm{BER}_{\mathrm{DbRS}}^{\mathrm{Up}} &= \tfrac{\theta\sqrt{\vartheta}K}{2}+\textstyle\sum_{k=1}^{K}\sum_{t=0}^{n(m_2-1)}\sum_{n=1}^{N_k}\binom{N_k}{n}\frac{(-1)^n b_t^n}{\Gamma(m_1M)} \\
&\times\frac{n^{-t}\theta\sqrt{\vartheta}}{\sqrt{\pi}}\left(\tfrac{m_1\lambda_{E,k}nm_2\lambda_{D,k}}{\chi_k\bar{\gamma}_P}\right)^{\frac{m_1M+t}{2}}\int_0^\infty x^{\frac{m_1M+t-1}{2}} \\
&\times\exp(-x)\quad K_{m_1M-t}\left(2\sqrt{\tfrac{m_1\lambda_{E,k}nm_2\lambda_{D,k}x}{\chi_k\bar{\gamma}_P}}\right)dx. \qquad (61)
\end{aligned}$$

By changing variable $y=\sqrt{x}$, equation (61) can be expressed as

$$\begin{aligned}
\mathrm{BER}_{\mathrm{DbRS}}^{\mathrm{Up}} &= \frac{\theta\sqrt{\vartheta}K}{2}+\sum_{k=1}^{K}\sum_{t=0}^{m_2-1}\sum_{n=1}^{N_k}(-1)^n\binom{N_k}{n}\frac{2b_t^n\theta\sqrt{\vartheta}}{\Gamma(m_1M)} \\
&\times\frac{n^{-t}}{\sqrt{\pi}}\left(\frac{m_1\lambda_{E,k}nm_2\lambda_{D,k}}{\chi_k\bar{\gamma}_P}\right)^{\frac{m_1M+t}{2}}\int_0^\infty y^{m_1M+t} \\
&\times\exp(-y^2)K_{m_1M-t}\left(2y\sqrt{\frac{m_1\lambda_{E,k}nm_2\lambda_{D,k}}{\chi_k\bar{\gamma}_P}}\right)dy. \qquad (62)
\end{aligned}$$

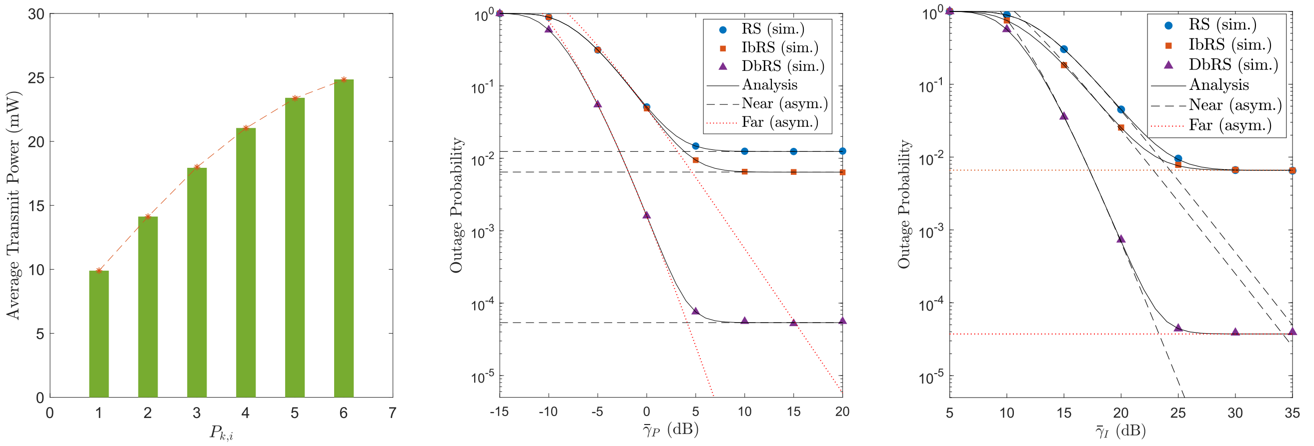

(a) Average transmit power versus $P_{k,i}$, with $\bar{\gamma}_I = 20$ dB and $\bar{\gamma}_P = 2$ dB

(b) The system OP versus $\bar{\gamma}_I$ in dB with $\bar{\gamma}_I = 20$ dB

(c) The system OP versus $\bar{\gamma}_P$ in dB with $\bar{\gamma}_P = 2$ dB

FIGURE 3. Average transmit power versus $P_{k,i}$, and the system OP versus $\bar{\gamma}_P$ and $\bar{\gamma}_I$.

By applying [27, Eq. (6.631.3)] for the corresponding integrals in (62), we can obtain the desired result as (59). The proof is concluded. ■

IV. NUMERICAL RESULTS

In this section, we present illustrative numerical examples for the achievable performance of the proposed relay selection schemes. Monte-Carlo simulations results are also provided to verify the analytical expressions. We consider a bi-dimensional plane, where the distance between sources and destinations as 10 meters, i.e., $d_{\mathsf{SD}} = 10$ m, the reference distance as 1 meter, i.e., $d_0 = 1$ m, and the pathloss at d_0 is $\mathcal{L} = -30$ dB. The position of S, $\mathsf{R}_{k,i}$, D, PB_m and PR are $(0, 0)$, $(k/K, 0)$, $(10, 0)$, $(7.0, 5.0)$ and $(7.0, -5.0)$, respectively. Unless otherwise stated, we set in all simulations the pathloss exponent $\beta = 3$, the shape parameters $m_1 = 2$, $m_2 = 2$ and $m_3 = 2$, the energy conversion efficiency $\eta = 0.8$, the target data rate $R_{th} = 1$ bits/s/Hz, the number of antennas at PR $L = 2$, the number of antennas at PB $M = 3$, number of hops $K = 6$, and the number of relays in each cluster $N_k = 2$, and the noise variance is normalized as $\sigma^2 = 1$.

We first present the proposed *harvest and accumulate* energy model by plotting the average transmit power in mW for the six-hop in secondary multi-hop network as shown in Fig. 3. As can be observed, the average transmit power at each relay node is monotonically increasing indicating that the latter relay nodes have more opportunities to harvest and accumulate energies to guarantee their data transmission. This results are consistent with the original intention of the proposed energy model which is analyzed in (1). It also ensures that the relay nodes are sufficient energy to perform data transmission subject to the minimum power constraint in cognitive wireless powered relaying networks.

We now study the system outage performance of all schemes versus $\bar{\gamma}_P$ in dB as shown in Fig. 3b. The value

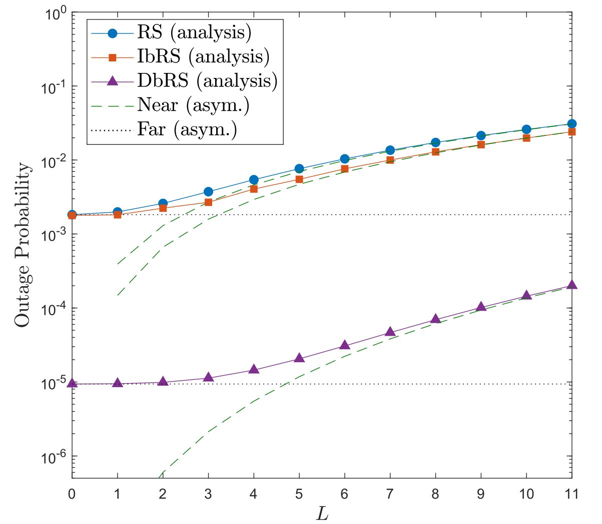

FIGURE 4. Effects of number of antennas at PR on the system OP with $\bar{\gamma}_I = 25$ dB and $\bar{\gamma}_P = 10$ dB.

of average SNR $\bar{\gamma}_P$ is varied while that of $\bar{\gamma}_I$ is fixed. As expected, when the average SNR $\bar{\gamma}_P$ is increased, the OP of all schemes is significantly improved. The reason is that increasing the average SNR can provide higher energy harvested at communication nodes for supporting data transmission. At the high range of $\bar{\gamma}_P$, the OP of all schemes are converged to their error-floor levels. This results can be explained by considering the fact that when $\bar{\gamma}_P$ is large enough, the transmit power at each secondary node in (4) is the upper bounded by the peak interference power constraint I_p which also confirms the accurate analytical approaches of the near scenario in Subsection III-B. In Fig. 3c, we vary the value of $\bar{\gamma}_I$ while the average SNR $\bar{\gamma}_I$ is fixed. The DbRS scheme again shows its superiority over other existing schemes. At high value of $\bar{\gamma}_I$, all schemes converge to their outage floors, which correctly validates the performance

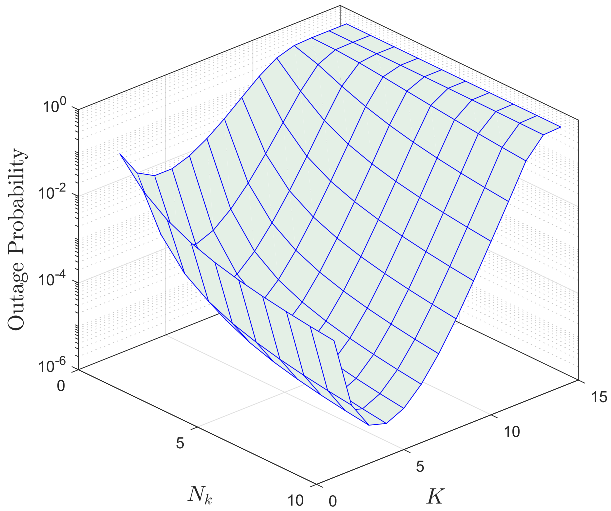

FIGURE 5. Effects of N_k and K on the OP of DbRS scheme with $\bar{\gamma}_I = 20$ dB and $\bar{\gamma}_P = 3$ dB.

analysis approaches of the far scenario. It can be further noticed that DbRS and IbRS schemes require more CSI estimations than that of RS one, which causes slight complexity for implementing in practice. However, DbRS and IbRS schemes provide the better reception reliability compared to RS scheme. In addition, Fig. 3b and Fig. 3c also present that the theoretical and simulation results are in excellent agreement confirming the correctness of our derivation approach.

We now shift our focus to the effect of number of antennas at PR, L, on the system OP as shown in Fig. 4. As can be observed, when L is large, the OP of secondary multi-hop network is gradually increased and convergences to that of the near scenario. An interesting observation drawn from this figure is that the system performance trends and behaviors are completely unfolded through the asymptotic results. Particularly, in DbRS scheme, when L is relatively small, i.e. L is less than 4, the system OP in far scenario is a function of L while on the other hands, when L becomes large, i.e. L is greater than 4, the system OP in near scenario is a function of L. A similar observation can be found in RS and IbRS schemes. These asymptotic results can reduce much complexity to make the system simpler to implement in the practice, and are excellently suitable for network planning and design. A further conclusion can be confirmed in Figs. 3b, 3c, and 4 that the DbRS scheme outperforms IbRS scheme, which in turns outperforms RS scheme. Thus, we turn our focus to the effects of related parameters on the performance of DbRS scheme in the following figures to provide some interesting insights into the system characteristics and behaviors.

Fig. 5 plots the system OP as a function of the number of relays, N_k, and the number of hops, K. As can be observed, the improvement of the system OP will be proportional to the number of relays in each cluster since more relays taking part in relay selection process can improve the end-to-end SNR. Moreover, the system OP is a convex function of K and there exists an optimal number of hops that minimizes the system OP. For example, the optimal number of hops is 5 for DbRS scheme with any value of N_k. Specifically, the system performance is degraded when the number of hops is increased due to the pathloss effect, as expected.

Fig. 6a investigates the effects of the time switching α on the system outage performance. As can be observed, the target data rate R_{th} impacts significantly on the system performance and there exists optimum values of α that minimizes the system OP. Specifically, when R_{th} are set to 0.1, 0.3, 0.6, and 1.0 bps/Hz, the optimum values are changed approximately 0.1, 0.2, 0.3, and 0.37, respectively. This results can be explained by considering the fact that when the target data rate is increased, the secondary multi-hop network requires more time for data transmission resulting the decrease of energy harvesting time.

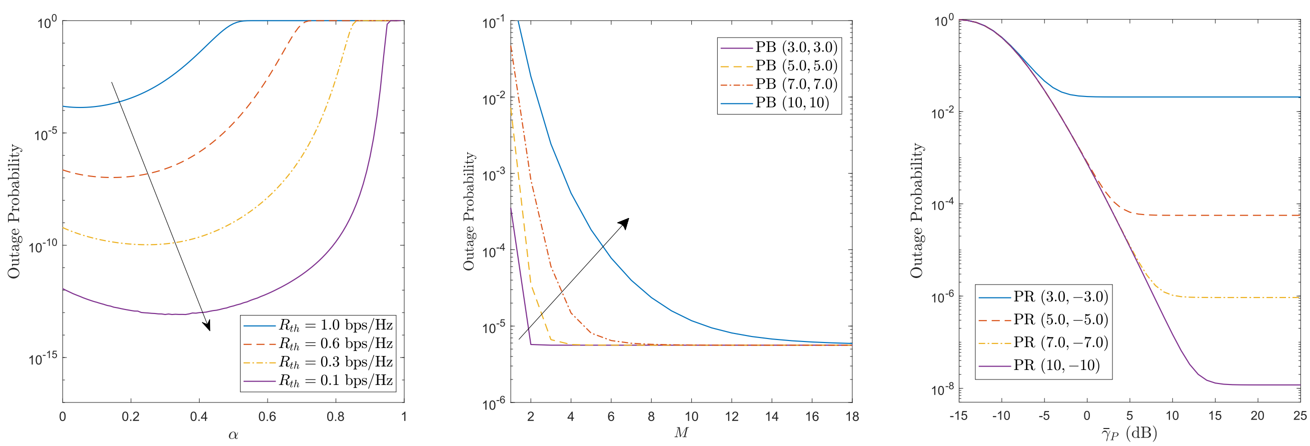

(a) Effect of α on the system OP under different data rates R_{th}, with $\bar{\gamma}_I = 20$ dB and $\bar{\gamma}_P = 5$ dB

(b) Effect of the number of antennas at the PB on the system OP under different PB placement scenarios, with $\bar{\gamma}_I = 20$ dB and $\bar{\gamma}_P = 5$ dB

(c) Effect of the PR placement scenarios on the system OP with $\bar{\gamma}_I = 20$ dB

FIGURE 6. Effects of related parameters on the system outage probability.

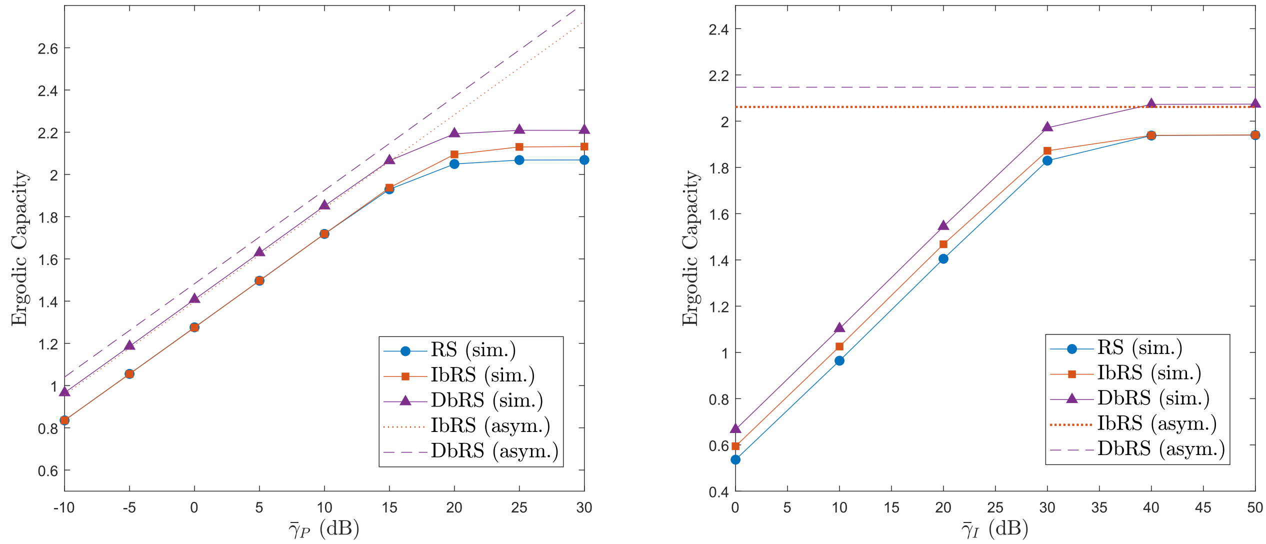

(a) Ergodic capacity versus $\bar{\gamma}_P$ in dB, with $\bar{\gamma}_I = 35$ dB

(b) Ergodic capacity versus $\bar{\gamma}_I$ in dB, with $\bar{\gamma}_P = 15$ dB

FIGURE 7. Exact ergodic capacity of three schemes and its corresponding upper bound versus $\bar{\gamma}_P$ and $\bar{\gamma}_I$ in dB.

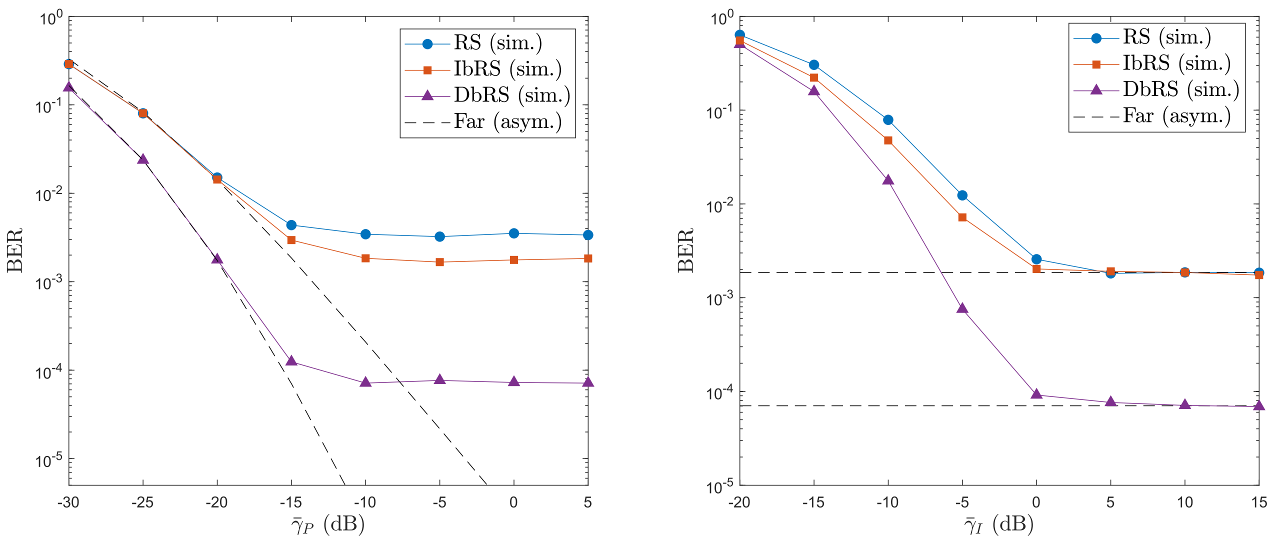

(a) Average BER versus $\bar{\gamma}_P$ in dB with $\bar{\gamma}_I = -2$ dB

(b) Average BER versus $\bar{\gamma}_I$ in dB with $\bar{\gamma}_P = -15$ dB

FIGURE 8. Average BER of three schemes and its corresponding upper bound against $\bar{\gamma}_P$ and $\bar{\gamma}_I$ in dB.

We now direct our attention to the effect of number of antennas at PB on the system outage performance under different PB placement scenarios as shown in Fig. 6b. As can be observed, the enhancement of system OP is proportional to the number of antennas at PB. Deploying more antennas at the PB can provide higher energy radiation resulting in more energy harvested at communication nodes for supporting data transmission. Moreover, when the position of PB is gradually far away from multi-hop network, the system performance is degraded due to the pathloss effect. Finally, the outage floors occur in all PB placement scenarios because the transmit power of each relay transmitter is always constrained as (4).

In Fig. 6c, the PR placement also imposes considerable effects on the system outage performance. As can be seen, when PR is located father away from secondary multi-hop network, the system OP is enhanced because the transmit power at each relay in (4) now is the upper bounded by the harvested power constraint P_k^E and can be increased proportionally to P_k^E without interfering to PR. However, the system OP is converged to different outage floors in high $\bar{\gamma}_P$ because the transmit power of each relay is constrained by (4) with the upper bounded by the interference I_p.

Figs. 7a and 7b show the ergodic capacity (EC) of each scheme versus $\bar{\gamma}_P$ and $\bar{\gamma}_I$ in dB, respectively. Again, the DbRS shows its superior compared to that of IbRS and RS schemes. As shown in 7a, the IbRS scheme outperforms RS scheme in the relative high average SNRs $\bar{\gamma}_P$ while they have the same EC performance at low region of $\bar{\gamma}_P$. The reason is that the maximum transmit power at each relay node in (4) is the upper bound by $\bar{\gamma}_P$ and be unaffected by the interference channel based relay selection in IbRS scheme resulting in the same capacity performance. On the other hand, the transmit power at each relay node is the upper bound by $\bar{\gamma}_I$ and the interference channel based relay selection in IbRS scheme shows its advantage compared to the RS scheme in Fig. 7b. Moreover, the asymptotic results indicate the tightness upper bound for the ergodic capacity of each scheme in the far scenario confirming the correctness of our approximation approaches. Specifically, the upper bound of DbRS gets tighter than that of IbRS and RS schemes. For example, in Fig. 7a, the gaps between these upper bounds in IbRS and DbRS schemes at 15 dB are about 1.25 and 2 dB, respectively.

Figs. 8a and 8b sketch the average BER performance of the proposed schemes for the BPSK modulation against the average SNR $\bar{\gamma}_P$ and $\bar{\gamma}_I$, respectively. As can be observed, average BER results are the counterpart of the ergodic capacity results shown in Fig. 7. The asymptotic results are also plotted to validate correctly the average BER behavior of all schemes in the far scenario. As expected, when $\bar{\gamma}_P$ or $\bar{\gamma}_I$ is increased, the average BER performance is improved. Particularly, in Fig. 8a, at very low value of $\bar{\gamma}_P$, the transmit power in (4) is very small resulting in large BER. For example, at $\bar{\gamma}_P = -25$ dB, the average BER values of DbRS and IbRS schemes are about 0.0125 and 0.08 for BPSK, respectively. When $\bar{\gamma}_P$ is high enough, the transmit power is constrained by the minimum value in (4) resulting in the convergence of average BER to an error-floor. A similar observation can also be found for all schemes at high value of $\bar{\gamma}_I$ in Fig. 8b, where the asymptotic results are served as the upper bounds of the end-to-end average BER. Finally, BER performance is also a function of $\bar{\gamma}_P$ and $\bar{\gamma}_I$ at their high regions.

V. CONCLUSION

In this paper, we proposed the interference and data channels based relay selections to improve the end-to-end performance for cognitive wireless powered multi-hop relaying networks in terms of outage probability, ergodic capacity and average BER over Nakagami-m fading channels. Particularly, the outage performance results were analyzed under two practical scenarios such as near and far scenarios, providing simple forms of analysis suitable for network planning and design. The numerical results presented that the data channel based relay selection, i.e., DbRS scheme, always outperformed interference channel based relay selection, i.e., IbRS scheme, which by its turn outperformed RS scheme for the same channel setting. Moreover, the secondary multi-hop network performance was improved by appropriately designing the target data rate, time switching ratio, number of relays in each cluster, the number of antennas at PB and PR and their placements. Finally, the proposed cognitive wireless powered multi-hop relaying system could be a promising scheme for future wireless sensor networks to enhance the system performance and extend the network coverage.

APPENDIX A
PROOF OF THEOREM 1

We start the proof by considering the OP of the RS scheme which can be rewritten from (11) as

$$\mathcal{P}_{\text{out}}^{\text{RS}} = 1 - \prod_{k=1}^{K}\left[1 - F_{\gamma_k^{\text{RS}}}(\gamma_{\text{th}})\right] \tag{63}$$

For the sake of notational convenience, let $X = \|\mathbf{g}_k\|^2 = \sum_{m=1}^{M}|g_{m,k,i}|^2$, $Y = |h_{k,i^*,j}|^2$ and $Z = \sum_{l=1}^{L}|f_{k,i^*,l}|^2$. From (6), the CDF of γ_k^{RS} can be written as

$$F_{\gamma_k^{\text{RS}}}(\gamma_{\text{th}}) = \underbrace{\Pr[\chi_k\bar{\gamma}_P X < \bar{\gamma}_I/Z, \chi_k\bar{\gamma}_P XY < \gamma_{\text{th}}]}_{I_1} + \underbrace{\Pr[\chi_k\bar{\gamma}_P X > \bar{\gamma}_I/Z, \bar{\gamma}_I Y/Z < \gamma_{\text{th}}]}_{I_2}. \tag{64}$$

In order to obtain $F_{\gamma_k^{\text{RS}}}(\gamma_{\text{th}})$, we need to calculate I_1 and I_2. We first consider I_1 which can be rewritten as

$$I_1 = \int_0^\infty F_Z\left(\frac{\bar{\gamma}_I}{\chi_k\bar{\gamma}_P x}\right)F_Y\left(\frac{\gamma_{\text{th}}}{\chi_k\bar{\gamma}_P x}\right)f_X(x)dx, \tag{65}$$

Recalling that X is the summation of M i.i.d. gamma distributed random variables (RVs), thus it follows the chi-square distribution. Assuming m_1 integer, the PDF and CDF of X are given, respectively, as [36]

$$f_X(x) = \frac{(m_1\lambda_{E,k})^{m_1M}x^{m_1M-1}}{\Gamma(m_1M)}\exp(-m_1\lambda_{E,k}x), \tag{66}$$

$$F_X(x) = 1 - \exp(-m_1\lambda_{E,k}x)\sum_{t=0}^{m_1M-1}\frac{(m_1\lambda_{E,k}x)^t}{t!}. \tag{67}$$

Similar to the distribution of X, Z is the summation of L i.i.d. gamma distributed RVs; thus, the PDF and CDF of Z are given, respectively, as

$$f_Z(x) = \frac{(m_3\lambda_{I,k})^{m_3L}x^{m_3L-1}}{\Gamma(m_3L)}\exp(-m_3\lambda_{I,k}x), \tag{68}$$

$$F_Z(x) = 1 - \exp(-m_3\lambda_{I,k}x)\sum_{v=0}^{m_3L-1}\frac{(m_3\lambda_{I,k}x)^t}{t!}. \tag{69}$$

Then, plugging $F_Z(\cdot)$, $f_X(\cdot)$, and the CDF of Y, i.e.,

$$F_Y(x) = 1 - \exp(-m_2\lambda_{D,k}x)\sum_{u=0}^{m_2-1}\frac{(m_2\lambda_{D,k}x)^u}{u!}, \tag{70}$$

into (65), along with the help of [27, Eq. (3.471.9)] and after some manipulations, the closed-form expression of I_1 can be obtained as

$$I_1 = 1 - \sum_{u=0}^{m_2-1} \frac{2}{\Gamma(m_1 M) u!} \left(\frac{m_1 \lambda_{E,k} m_2 \lambda_{D,k} \gamma_{\text{th}}}{\chi_k \bar{\gamma}_P} \right)^{\frac{m_1 M+u}{2}} \times K_{m_1 M-u}\left(2\sqrt{\frac{m_1 \lambda_{E,k} m_2 \lambda_{D,k} \gamma_{\text{th}}}{\chi_k \bar{\gamma}_P}}\right) - \sum_{v=0}^{m_3 L-1} \frac{2}{v!} \times \frac{1}{\Gamma(m_1 M)} \left[\left(\frac{m_1 \lambda_{E,k} m_3 \lambda_{I,k} \bar{\gamma}_I}{\chi_k \bar{\gamma}_P} \right)^{\frac{m_1 M+v}{2}} \times K_{m_1 M-v}\left(2\sqrt{\frac{m_1 \lambda_{E,k} m_3 \lambda_{I,k} \bar{\gamma}_I}{\chi_k \bar{\gamma}_P}}\right) - \sum_{u=0}^{m_2-1} \frac{1}{u!} \times \left(\frac{m_1 \lambda_{E,k}}{\chi_k \bar{\gamma}_P} \right)^{\frac{m_1 M+v+u}{2}} \frac{(m_3 \lambda_{I,k} \bar{\gamma}_I + m_2 \lambda_{D,k} \gamma_{\text{th}})^{\frac{m_1 M-v-u}{2}}}{(m_3 \lambda_{I,k} \bar{\gamma}_I)^{-v} (m_2 \lambda_{D,k} \gamma_{\text{th}})^{-u}} \times K_{m_1 M-v-u}\left(2\sqrt{\frac{m_1 \lambda_{E,k}(m_3 \lambda_{I,k} \bar{\gamma}_I + m_2 \lambda_{D,k} \gamma_{\text{th}})}{\chi_k \bar{\gamma}_P}}\right) \right]. \tag{71}$$

We are now in a position to derive I_2, which can be rewritten under the form as

$$I_2 = \int_0^\infty \left[1 - F_X\left(\frac{\bar{\gamma}_I}{\chi_k \bar{\gamma}_P x}\right)\right] F_Y\left(\frac{\gamma_{\text{th}} x}{\bar{\gamma}_I}\right) f_Z(x) dx. \tag{72}$$

Substituting $F_X(\cdot)$, $f_Z(\cdot)$ and $F_Y(\cdot)$ into (72), along with the help of [27, Eq. (3.471.9)] and after some manipulations, I_2 can be obtained as

$$I_2 = 1 - \sum_{t=0}^{m_1 M-1} \frac{2}{\Gamma(m_3 L) t!} \left[\left(\frac{m_1 \lambda_{E,k} m_3 \lambda_{I,k} \bar{\gamma}_I}{\chi_k \bar{\gamma}_P} \right)^{\frac{m_3 L+t}{2}} \times K_{m_3 L-t}\left(2\sqrt{\frac{m_1 \lambda_{E,k} m_3 \lambda_{I,k} \bar{\gamma}_I}{\chi_k \bar{\gamma}_P}}\right) - \sum_{u=0}^{m_2-1} \frac{1}{u!} \times \left(\frac{m_1 \lambda_{E,k}}{\chi_k \bar{\gamma}_P} \right)^{\frac{m_3 L+u+t}{2}} \frac{(m_3 \lambda_{I,k} \bar{\gamma}_I + m_2 \lambda_{D,k} \gamma_{\text{th}})^{\frac{t-m_3 L-u}{2}}}{(m_3 \lambda_{I,k} \bar{\gamma}_I)^{-m_3 L} (m_2 \lambda_{D,k} \gamma_{\text{th}})^{-u}} \times K_{m_3 L+u-t}\left(2\sqrt{\frac{m_1 \lambda_{E,k}(m_3 \lambda_{I,k} \bar{\gamma}_I + m_2 \lambda_{D,k} \gamma_{\text{th}})}{\chi_k \bar{\gamma}_P}}\right) \right]. \tag{73}$$

Finally, by substituting I_1 and I_2 into (64), we can obtain the desired OP as (12). The proof of Theorem 1 is concluded.

APPENDIX B
PROOF OF LEMMA 1

The CDF of X_i^* can be rewritten as

$$F_{Z_i^*}(x) = \Pr\left(\min_{i=1,\ldots,N_k} Z_i < x\right) = 1 - \Pr\left(\min_{i=1,\ldots,N_k} Z_i > x\right) = 1 - \prod_{i=1}^{N_k} [1 - F_{Z_i}(x)]. \tag{74}$$

Plugging (69) into (74) which yields

$$F_{Z_i^*}(x) = 1 - \prod_{i=1}^{N_k} \exp(-m_3 \lambda_{I,k} N_k x) \left[\sum_{v=0}^{m_3 L-1} \frac{(m_3 \lambda_{I,k} x)^v}{v!} \right]. \tag{75}$$

By using [27, Eq. 0.314], the CDF of Z_i^* can be obtained as (15). Next, we derive the PDF of Z_i^* by firstly rewriting its CDF from (74) in the form as

$$F_{Z_i^*}(x) = 1 - \prod_{i=1}^{N_k} \left[1 - \frac{\gamma(m_3 L, m_3 \lambda_{I,k} x)}{\Gamma(m_3 L)} \right]. \tag{76}$$

By taking the derivative of (76), we obtain the PDF of Z_i^* as

$$f_{Z_i^*}(x) = \prod_{i=1}^{N_k-1} \left[1 - \frac{\gamma(m_3 L, m_3 \lambda_{I,k} x)}{\Gamma(m_3 L)} \right] \frac{N_k (m_3 \lambda_{I,k})^{m_3 L}}{\Gamma(m_3 L)} \times x^{m_3 L-1} \exp(-m_3 \lambda_{I,k} x) = \prod_{i=1}^{N_k-1} \left[\sum_{v=0}^{m_3 L-1} \frac{(m_3 \lambda_{I,k} x)^v}{v!} \right] \frac{N_k (m_3 \lambda_{I,k})^{m_3 L}}{\Gamma(m_3 L)} \times x^{m_3 L-1} \exp(-m_3 \lambda_{I,k} N_k x). \tag{77}$$

Again, we apply [27, Eq. 0.314] for (77), the PDF of Z_i^* can be obtained as (16). The proof of Lemma 1 is concluded.

APPENDIX C
PROOF OF THEOREM 4

We first consider the asymptotic expressions for the OP of RS scheme by making use of the fact that $\prod_{k=1}^{K}(1 - x^k) \approx 1 - \sum_{k=1}^{K} x_k$ for small x_k. From (63), the asymptotic expression for the OP of RS scheme can be asymptotically expressed as

$$\mathcal{P}_{\text{asym}}^{\text{RS}} \approx \sum_{k=1}^{K} F_{\gamma_k^{\text{RS}}}(\gamma_{\text{th}}). \tag{78}$$

Next, we consider the far scenario with $I_p \to \infty$. From (31), the transmit power is approximated as $P_k \approx \chi_k P \|\mathbf{g}_k\|^2$, and the instantaneous SNR can be expressed as $\gamma_{k,F}^{\text{RS}} = \chi_k \bar{\gamma}_P \|\mathbf{g}_k\|^2 |h_{k,i^*,j^*}|^2$. Let $X = \|\mathbf{g}_k\|^2 = \sum_{m=1}^{M} |g_{m,k,i}|^2$ and $Y = |h_{k,i^*,j}|^2$, the CDF of $\gamma_{k,F}^{\text{RS}}$ can be calculated as

$$F_{\gamma_{k,F}^{\text{RS}}}(\gamma_{\text{th}}) = \int_0^\infty F_Y\left(\frac{\gamma_{\text{th}}}{\chi_k \bar{\gamma}_P x}\right) f_X(x) dx, \tag{79}$$

Plugging $F_Y(\cdot)$ and $f_X(\cdot)$ into (79), along with the help of [27, Eq. (3.471.9)], we can obtain the desired result as (33).

For the near scenario with $P \to \infty$, the transmit power is approximated as $P_k \approx \bar{\gamma}_I / \sum_{l=1}^{L} |f_{k,i,l}|^2$, and the instantaneous SNR is expressed as $\gamma_{k,N}^{\text{RS}} = \bar{\gamma}_I |h_{k,i^*,j^*}|^2 / \sum_{l=1}^{L} |f_{k,i,l}|^2$. Let $Z = \sum_{l=1}^{L} |f_{k,i^*,l}|^2$, the CDF of $\gamma_{k,N}^{\text{RS}}$ can be calculated as

$$F_{\gamma_{k,N}^{\text{RS}}}(\gamma_{\text{th}}) = \int_0^\infty F_Y\left(\frac{\gamma_{\text{th}} x}{\bar{\gamma}_I}\right) f_Z(x) dx, \tag{80}$$

Plugging $F_Y(\cdot)$ and $f_Z(\cdot)$ into (80), and after some algebraic manipulations, we can obtain the desired result as (34). From $F_{\gamma_{k,F}^{\text{RS}}}(\gamma_{\text{th}})$ and $F_{\gamma_{k,N}^{\text{RS}}}(\gamma_{\text{th}})$ and plugging them into (78), we obtain the results as (32). The proof is concluded.

APPENDIX D
PROOF OF THEOREM 5

First, the asymptotic expressions for the OP of IbRS scheme can be expressed as

$$\mathcal{P}_{\rm asym}^{\rm IbRS} \approx \sum_{k=1}^{K} F_{\gamma_k^{\rm IbRS}}(\gamma_{\rm th}). \tag{81}$$

Next, we consider the near scenario with $P \to \infty$, the transmit power is approximated as $P_k \approx \bar{\gamma}_I / \min\limits_{i=1,\ldots,N_k} \sum_{l=1}^{L} |f_{k,i,l}|^2$, and the instantaneous SNR is expressed as $\gamma_{k,N}^{\rm IbRS} = \bar{\gamma}_I |h_{k,i,j^*}|^2 / \min\limits_{i=1,\ldots,N_k} \sum_{l=1}^{L} |f_{k,i,l}|^2$. Let $Z = \min\limits_{i=1,\ldots,N_k} \sum_{l=1}^{L} |f_{k,i^*,l}|^2$, the CDF of $\gamma_{k,N}^{\rm IbRS}$ is calculated as

$$F_{\gamma_{k,N}^{\rm RS}}(\gamma_{\rm th}) = \int_0^\infty F_Y\Big(\frac{\gamma_{\rm th} x}{\bar{\gamma}_I}\Big) f_Z(x) dx, \tag{82}$$

Plugging $F_Y(\cdot)$ and $f_Z(\cdot)$ into (82), and after some algebraic manipulations, we can obtain the desired result as (37),s which completes the proof.

APPENDIX E
PROOF OF THEOREM 6

The asymptotic expressions for the OP of DbRS scheme can be expressed as

$$\mathcal{P}_{\rm asym}^{\rm DbRS} \approx \sum_{k=1}^{K} F_{\gamma_k^{\rm DbRS}}(\gamma_{\rm th}). \tag{83}$$

Next, we consider the far scenario with $I_p \to \infty$ and the transmit power is approximated as $P_k \approx \chi_k P \|\mathbf{g}_k\|^2$. The instantaneous SNR can be expressed as $\gamma_{k,F}^{\rm RS} = \max\limits_{j=1,\ldots,N_{k+1}} \chi_k \bar{\gamma}_P \|\mathbf{g}_k\|^2 |h_{k,i^*,j}|^2$. Let $X = \|\mathbf{g}_k\|^2$ and $Y = \max\limits_{j=1,\ldots,N_{k+1}} |h_{k,i^*,j}|^2$, the CDF of $\gamma_{k,F}^{\rm DbRS}$ is calculated as

$$F_{\gamma_{k,F}^{\rm DbRS}}(\gamma_{\rm th}) = \int_0^\infty F_Y\Big(\frac{\gamma_{\rm th}}{\chi_k \bar{\gamma}_P x}\Big) f_X(x) dx, \tag{84}$$

Plugging $F_Y(\cdot)$ and $f_X(\cdot)$ into (84), along with the help of [27, Eq. (3.471.9)], we can obtain the desired result as (39).

For the near scenario with $P \to \infty$, the transmit power is approximated as $P_k \approx \bar{\gamma}_I / \sum_{l=1}^{L} |f_{k,i,l}|^2$, and the instantaneous SNR is expressed as $\gamma_{k,N}^{\rm DbRS} = \max\limits_{j=1,\ldots,N_{k+1}} \bar{\gamma}_I |h_{k,i^*,j}|^2 / \sum_{l=1}^{L} |f_{k,i,l}|^2$. Let $Z = \sum_{l=1}^{L} |f_{k,i^*,l}|^2$, the CDF of $\gamma_{k,N}^{\rm DbRS}$ can be calculated as

$$F_{\gamma_{k,N}^{\rm DbRS}}(\gamma_{\rm th}) = \int_0^\infty F_Y\Big(\frac{\gamma_{\rm th} x}{\bar{\gamma}_I}\Big) f_Z(x) dx, \tag{85}$$

Plugging $F_Y(\cdot)$ and $f_Z(\cdot)$ into (85), and after some algebraic manipulations, we can obtain the desired result as (40). From $F_{\gamma_{k,F}^{\rm DbRS}}(\gamma_{\rm th})$ and $F_{\gamma_{k,N}^{\rm DbRS}}(\gamma_{\rm th})$ and plugging them into (83), we obtain the results as (38). The proof is concluded.

REFERENCES

[1] L. Mohjazi, M. Dianati, G. K. Karagiannidis, S. Muhaidat, and M. Al-Qutayri, "RF-powered cognitive radio networks: Technical challenges and limitations," *IEEE Commun. Mag.*, vol. 53, no. 4, pp. 94–100, Apr. 2015.

[2] D. Niyato, D. I. Kim, M. Maso, and Z. Han, "Wireless powered communication networks: Research directions and technological approaches," *IEEE Wireless Commun.*, vol. 24, no. 6, pp. 88–97, Dec. 2017.

[3] J. Ren, J. Hu, D. Zhang, H. Guo, Y. Zhang, and X. Shen, "RF energy harvesting and transfer in cognitive radio sensor networks: Opportunities and challenges," *IEEE Commun. Mag.*, vol. 56, no. 1, pp. 104–110, Jan. 2018.

[4] A. Goldsmith, S. A. Jafar, I. Maric, and S. Srinivasa, "Breaking spectrum gridlock with cognitive radios: An information theoretic perspective," *Proc. IEEE*, vol. 97, no. 5, pp. 894–914, Apr. 2009.

[5] I. Krikidis, S. Timotheou, S. Nikolaou, G. Zheng, D. W. K. Ng, and R. Schober, "Simultaneous wireless information and power transfer in modern communication systems," *IEEE Commun. Mag.*, vol. 52, no. 11, pp. 104–110, Nov. 2014.

[6] T. Q. Duong, P. L. Yeoh, V. N. Q. Bao, M. Elkashlan, and N. Yang, "Cognitive relay networks with multiple primary transceivers under spectrum-sharing," *IEEE Signal Process. Lett.*, vol. 19, no. 11, pp. 741–744, Nov. 2012.

[7] V. N. Q. Bao and T. Q. Duong, "Exact outage probability of cognitive underlay DF relay networks with best relay selection," *IEICE Trans. Commun.*, vol. E95.B, no. 6, pp. 2169–2173, Jun. 2012.

[8] P. L. Yeoh, M. Elkashlan, T. Q. Duong, N. Yang, and C. Leung, "Cognitive MIMO relaying in Nakagami-m fading," in *Proc. IEEE 77th Veh. Technol. Conf.*, Jun. 2013, pp. 1–5.

[9] Z. Wang, Z. Chen, B. Xia, L. Luo, and J. Zhou, "Cognitive relay networks with energy harvesting and information transfer: Design, analysis, and optimization," *IEEE Trans. Wireless Commun.*, vol. 15, no. 4, pp. 2562–2576, Apr. 2016.

[10] K. Huang and X. Zhou, "Cutting the last wires for mobile communications by microwave power transfer," *IEEE Commun. Mag.*, vol. 53, no. 6, pp. 86–93, Jun. 2015.

[11] C. Zhong, X. Chen, Z. Zhang, and G. K. Karagiannidis, "Wireless-powered communications: Performance analysis and optimization," *IEEE Trans. Commun.*, vol. 63, no. 12, pp. 5178–5190, Dec. 2015.

[12] Z. Hadzi-Velkov, I. Nikoloska, G. K. Karagiannidis, and T. Q. Duong, "Wireless networks with energy harvesting and power transfer: Joint power and time allocation," *IEEE Signal Process. Lett.*, vol. 23, no. 1, pp. 50–54, Jan. 2016.

[13] R. Zhang and C. K. Ho, "MIMO broadcasting for simultaneous wireless information and power transfer," *IEEE Trans. Wireless Commun.*, vol. 12, no. 5, pp. 1989–2001, May 2013.

[14] A. A. Nasir, X. Zhou, S. Durrani, and R. A. Kennedy, "Relaying protocols for wireless energy harvesting and information processing," *IEEE Trans. Wireless Commun.*, vol. 12, no. 7, pp. 3622–3636, Jul. 2013.

[15] N. T. Van, H. M. Tan, T. M. Hoang, T. T. Duy, and V. N. Q. Bao, "Exact outage probability of energy harvesting incremental relaying networks with MRC receiver," in *Proc. Int. Conf. Adv. Technol. Commun.*, Oct. 2016, pp. 120–125.

[16] V. N. Q. Bao, T. Q. Duong, and C. Tellambura, "On the performance of cognitive underlay multihop networks with imperfect channel state information," *IEEE Trans. Commun.*, vol. 61, no. 12, pp. 4864–4873, Dec. 2013.

[17] F. S. Al-Qahtani, R. M. Radaydeh, S. Hessien, T. Q. Duong, and H. Alnuweiri, "Underlay cognitive multihop MIMO networks with and without receive interference cancellation," *IEEE Trans. Commun.*, vol. 65, no. 4, pp. 1477–1493, Apr. 2017.

[18] H. K. Boddapati, M. R. Bhatnagar, and S. Prakriya, "Performance analysis of cluster-based multi-hop underlay CRNs using max-link-selection protocol," *IEEE Trans. Cogn. Commun. Netw.*, vol. 4, no. 1, pp. 15–29, Mar. 2018.

[19] J. Park, C. Jang, and J. H. Lee, "Outage analysis of underlay cognitive radio networks with multihop primary transmission," *IEEE Commun. Lett.*, vol. 20, no. 4, pp. 800–803, Apr. 2016.

[20] C. Xu, M. Zheng, W. Liang, H. Yu, and Y.-C. Liang, "Outage performance of underlay multihop cognitive relay networks with energy harvesting," *IEEE Commun. Lett.*, vol. 20, no. 6, pp. 1148–1151, Jun. 2016.

[21] C. Xu, M. Zheng, W. Liang, H. Yu, and Y. Liang, "End-to-end throughput maximization for underlay multi-hop cognitive radio networks with RF energy harvesting," *IEEE Trans. Wireless Commun.*, vol. 16, no. 6, pp. 3561–3572, Jun. 2017.

[22] N. T. Van, T. T. Duy, T. Hanh, and V. N. Q. Bao, "Outage analysis of energy-harvesting based multihop cognitive relay networks with multiple primary receivers and multiple power beacons," in *Proc. Int. Symp. Antennas Propag.*, Oct./Nov. 2017, pp. 1–2.
[23] E. Chen, M. Xia, D. B. D. Costa, and S. Aïssa "Multi-hop cooperative relaying with energy harvesting from cochannel interferences," *IEEE Commun. Lett.*, vol. 21, no. 5, pp. 1199–1202, May 2017.
[24] N. T. Van, T. N. Do, V. N. Q. Bao, and B. An, "Performance analysis of wireless energy harvesting multihop cluster-based networks over Nakagami-*m* fading channels," *IEEE Access*, vol. 6, pp. 3068–3084, Dec. 2017.
[25] V. N. Q. Bao, T. T. Duy, and N. T. Van, "Exact outage analysis of energy-harvesting multihop cluster-based networks with multiple power beacons over Nakagami-*m* fading channels," in *Proc. Int. Conf. Recent Adv. Signal Process., Telecommun. Comput.*, Jan. 2018, pp. 1–6.
[26] P. M. Nam, T. T. Duy, and P. Van Ca, "End-to-end security-reliability analysis of multi-hop cognitive relaying protocol with TAS/SC-based primary communication, total interference constraint and asymmetric fading channels," *Int. J. Commun. Syst.*, vol. 32, no. 2, p. e3854, Jan. 2019.
[27] I. S. Gradshteyn and I. M. Ryzhik, *Table of Integrals, Series, and Products*. New York, NY, USA: Academic, 2007.
[28] M. Abramowitz and I. A. Stegun, *Handbook of Mathematical Functions: With Formulas, Graphs, and Mathematical Tables*. Chelmsford, U.K: Courier Corp., 1972.
[29] A. Sgora, D. J. Vergados, and D. D. Vergados, "A survey of TDMA scheduling schemes in wireless multihop networks," *ACM Comput. Surv. (CSUR)*, vol. 47, no. 3, p. 53, 2015.
[30] P. N. Son and T. T. Duy, "Performance analysis of underlay cooperative cognitive full-duplex networks with energy-harvesting relay," *Comput. Commun.*, vol. 122, pp. 9–19, Jun. 2018.
[31] T. K. Y. Lo, "Maximum ratio transmission," in *Proc. IEEE Int. Conf. Commun.*, Vancouver, BC, Canada, vol. 2, Jun. 1999, pp. 1310–1314.
[32] A. Papoulis and S. U. Pillai, *Probability, Random Variables and Stochastic Processes*, 4th ed. New York, NY, USA: McGraw-Hill, 2002.
[33] T. M. Cover and A. A. El Gamal, "Capacity theorems for the relay channel," *IEEE Trans. Inf. Theory*, vol. 25, no. 5, pp. 572–584, Sep. 1979.
[34] G. Farhadi and N. C. Beaulieu, "On the ergodic capacity of multi-hop wireless relaying systems," *IEEE Trans. Wireless Commun.*, vol. 8, no. 5, pp. 2286–2291, May 2009.
[35] M. R. McKay, A. J. Grant, and I. B. Collings, "Performance analysis of MIMO-MRC in double-correlated Rayleigh environments," *IEEE Trans. Commun.*, vol. 55, no. 3, pp. 497–507, Mar. 2007.
[36] Z. Chen, Z. Chi, Y. Li, and B. Vucetic, "Error performance of maximal-ratio combining with transmit antenna selection in flat Nakagami-*m* fading channels," *IEEE Trans. Wireless Commun.*, vol. 8, no. 1, pp. 424–431, Jan. 2009.

TOAN-VAN NGUYEN received the B.S. degree in electronics and telecommunications engineering and the M.S. degree in electronics engineering from the Ho Chi Minh City University of Technology and Education, Vietnam, in 2011 and 2014, respectively. He is currently pursuing the Ph.D. degree in electronics and computer engineering at Hongik University, South Korea. His main research interests include wireless communications, energy harvesting, cooperative, and cognitive communications.

BEONGKU AN received the B.S. degree in electronic engineering from Kyungpook National University, South Korea, in 1988, the M.S. degree in electrical engineering from New York University (Polytechnic), New York City, NY, USA, in 1996, and the Ph.D. degree from the New Jersey Institute of Technology (NJIT), Newark, NJ, USA, in 2002. He joined the Faculty of the Department of Software and Communications Engineering, Hongik University, South Korea, where he is currently a Professor. From 1989 to 1993, he was a Senior Researcher with RIST, Pohang, South Korea. He was also a Lecturer and a RA in NJIT, from 1997 to 2002. His current research interests include mobile wireless networks and communications, such as ad-hoc networks, sensor networks, wireless cognitive radio networks, cellular networks, cooperative communication, multicast routing, QoS routing, energy harvesting, physical layer security, M2M/D2D, the IoT, visible light communication (VLC), cross-layer technology, 5G/Beyond 5G, NOMA, SWIPT, machine learning and block chain, and mobile cloud computing. He was the President of the IEIE Computer Society (The Institute of Electronics and Information Engineers, Computer Society), in 2012. Since 2013, he has been the General Chair in the International Conference, the International Conference on Green and Human Information Technology (ICGHIT). Prof. An was listed in Marquis Who's Who in Science and Engineering, and Marquis Who's Who in the World, respectively.